and Langtry, 1993). In Japan, many physicians prescribe low dose ZDV such as 400 mg/day to avoid drug-induced anemia and neutropenia even though the standard dose of ZDV is 500–600 mg/day in United States (Kimura et al., 1992, 1998). Given the dose-dependent nature of these adverse effects, they are concerned about increased risk of hematological toxicity using Combivir that contains 600 mg of ZDV as the daily dose for Japanese patients who have lower body weights compared to patients in United States. Moreover, long-term consequence of the hematological toxicity resulting from continuous use of Combivir has not been well defined. We retrospectively reviewed clinical records of HIV-1 infected cases under treatment of Combivir-containing regimen used in three hospitals in Japan and we analyzed clinical data cross-sectionally to evaluate long-term toxicity of Combivir.

2. Patients and methods

HIV-1 positive Japanese patients were recruited from Kumamoto University Hospital, Osaka National Hospital and International Medical Center of Japan from June 1999 (after the Combivir launch) until June 2003. The clinical record was investigated in a retrospective manner. All collected cases were separated into four groups, as follows;

Primary Combivir Group (PCV): started Combivir as a first-line HAART.
Secondary Combivir Group (SCV): changed to Combivir from other NRTIs.
Primary Control Group (PCO): started NRTIs (except for Combivir) as a first-line HAART.
Secondary Control Group (SCO): changed to NRTIs except Combivir from other NRTIs.

We checked hemoglobin levels and neutrophil counts to examine the influence on hematological toxicity of ZDV every 6 months. We analyzed the data that could be followed over 18 months for removing various biases such as drop out cases with abnormal laboratory test values. Moreover, we also checked the HIV-RNA, $CD4^+$ T-cell counts and other laboratory test data every 6 months. We also checked any adverse events. This study was done under the approval of the Institutional Review Board of the Kumamoto University Hospital, Japan. All participants provided written informed consent.

3. Results

3.1. Patients' characteristics

Of the 94 data on subjects were 55 who were on Combivir (PCV: 27, SCV: 28) and 39 were on control regimens (PCO: 29, SCO: 10). The NRTIs used in the control group included of 20 cases of ZDV (400 mg/day) + 3TC, 18 cases of stavudine (d4T) + 3TC and one case of d4T + didanosine (ddI). Patients' characteristics are shown in Table 1. A couple of factors are statistically different such as the sex ($p < 0.01$: Fisher's exact test), weight ($p < 0.05$: Student's t-test) and Karnofsky score ($p = 0.0062$: Student's t-test) between Combivir group and control group. Combivir was likely to be used for patients with a higher baseline weight and the males. The mean viral load at baseline in Combivir group was $10^{3.9}$ copies/mL and for the control group was $10^{4.1}$ copies/mL. There was no statistical difference between the groups. The baseline $CD4^+$ T-cell counts in Combivir group were higher than in the control group significantly ($393/mm^3$ versus $263/mm^3$; $p = 0.0101$: Student's t-test). Most patients were prescribed efavirenz (EFV) or nelfinavir (NFV) as a concomitant drug. Fifty-two percent of all patients were on EFV and 16% were taking NFV. The Combivir group had more combination cases with EFV than did the control group, because these two drugs approved for use in Japan at the same period have similar characteristics such as small pill counts and frequency of ingestion.

3.2. Effects on hemoglobin levels

To avoid biases in the data resulting from inclusion of patients with a shorter time follow up, including drop out cases, we focused on the patients that could be followed for over 18 months. Mean hemoglobin levels at baseline of Combivir group (PCV group: 13.9 g/dL, SCV group: 14.2 g/dL) were higher than for the control group (PCO group: 13.1 g/dL, SCO group: 13.7 g/dL) (Fig. 1A). It seems Combivir was likely to give to those with a lesser risk of anemia. We divided patients in PCV group into two sub-groups such as hemoglobin level decreased (sub-group A; $n = 10$) and not changed or increased (sub-group B: $n = 8$) at 6 months after starting Combivir. Fig. 1B shows a trend of hemoglobin levels in sub-group A. Each hemoglobin level at 6, 12, 18 and 24 months after starting treatment decreased significantly compared to baseline ($p < 0.005$, $p < 0.005$, $p < 0.005$ and $p < 0.05$, respectively; Wilcoxon matched pairs signed rank test). However, the decreased hemoglobin levels at 6 months gradually recovered to the baseline level despite continuation of the same regimen. The hemoglobin level at 18, 24 months increased significantly compared to 6-month values ($p < 0.05$ and $p < 0.005$, respectively). On the other hand, the hemoglobin level of sub-group B did not decrease for 18–30 months of follow up period (data not shown). The difference of background between sub-groups A and B was baseline level of hemoglobin and hematocrit. These levels in sub-group A were higher than for sub-group B statistically (14.9 ± 1.2 versus 12.6 ± 0.7; $p < 0.001$, 44.4 ± 3.2 versus 37.4 ± 2.0; $p < 0.001$, Student's t-test).

3.3. Effects on neutrophil counts

The trend of mean neutrophil counts was similar to counts for hemoglobin levels. Mean neutrophil counts of all groups

Table 1
Baseline characteristics

	Combivir group (PCV + SCV) (n = 55)	Control group (PCO + SCO) (n = 39)	p-value
Sex (male/female)	54/1	32/7	0.00815[a]
Age	35.9 ± 9.5 (22–68)	38.6 ± 10.7 (23–78)	0.2117[b]
Weight (kg)	64.6 ± 10.8 (47.0–91.6)	59.6 ± 11.2 (36.4–81.0)	0.0303[b]
Hemophilia			0.562[a]
Non	48	32	
A	5	7	
B	2	0	
Baseline VL (log)			0.4432[b]
<2.6	19	11	
2.6–3	1	1	
3–4	6	4	
4–5	11	13	
>5	15	10	
Unknown	3	0	
Mean ± S.D.	3.9 ± 1.2	4.1 ± 1.2	
Range	2.6–5.9	2.6–5.9	
Baseline CD4 count			0.0101[b]
<200	14	14	
200–500	25	19	
>500	13	5	
Unknown	3	1	
Mean ± S.D.	393 ± 265	263 ± 179	
Range	1–1132	5–607	
CDC class			0.8064[c]
A1	5	3	
A2	22	17	
A3	6	13	
B1	2	0	
B2	3	0	
B3	2	5	
C1	3	0	
C3	12	11	
Karnofsky score			0.0062[b]
20%	0	1	
40%	0	2	
50%	0	1	
60%	1	0	
70%	0	1	
80%	4	6	
90%	11	8	
100%	39	20	
Mean ± S.D.	95.8 ± 7.9	87.7 ± 19.4	

[a] Fisher' exact test.
[b] Student's t-test.
[c] Wilcoxon 2-sample test.

were over 2000/mm^3 and did not have statistically change from the baseline during the follow up period (Fig. 1C). We separated subjects in the PCV group into two sub-groups as well as for hemoglobin levels to examine the toxicity of Combivir to neutrophils. In the sub-group C (n = 10) those with mean neutrophil counts decreased and the sub-group D (n = 7) included subjects with no changes or increased neutrophil counts at 6 months after being on Combivir. Fig. 1D shows the trend of the neutrophil counts in sub-group C. Neutrophil counts at 6, 12, 18 and 24 months after starting the treatment decreased significantly compared to baseline ($p < 0.005$, $p < 0.05$, $p < 0.05$ and $p < 0.05$, respectively; Wilcoxon matched pairs signed rank test). However, the decreased neutrophil counts gradually recovered as did hemoglobin levels. The mean neutrophil counts at 18 months increased significantly compared to data at 6 months ($p < 0.05$; Wilcoxon matched pairs signed rank test).

3.4. Effects on other laboratory test value

MCV values at baseline for the secondary treatment group such as SCV group and SCO group were higher than for pri-

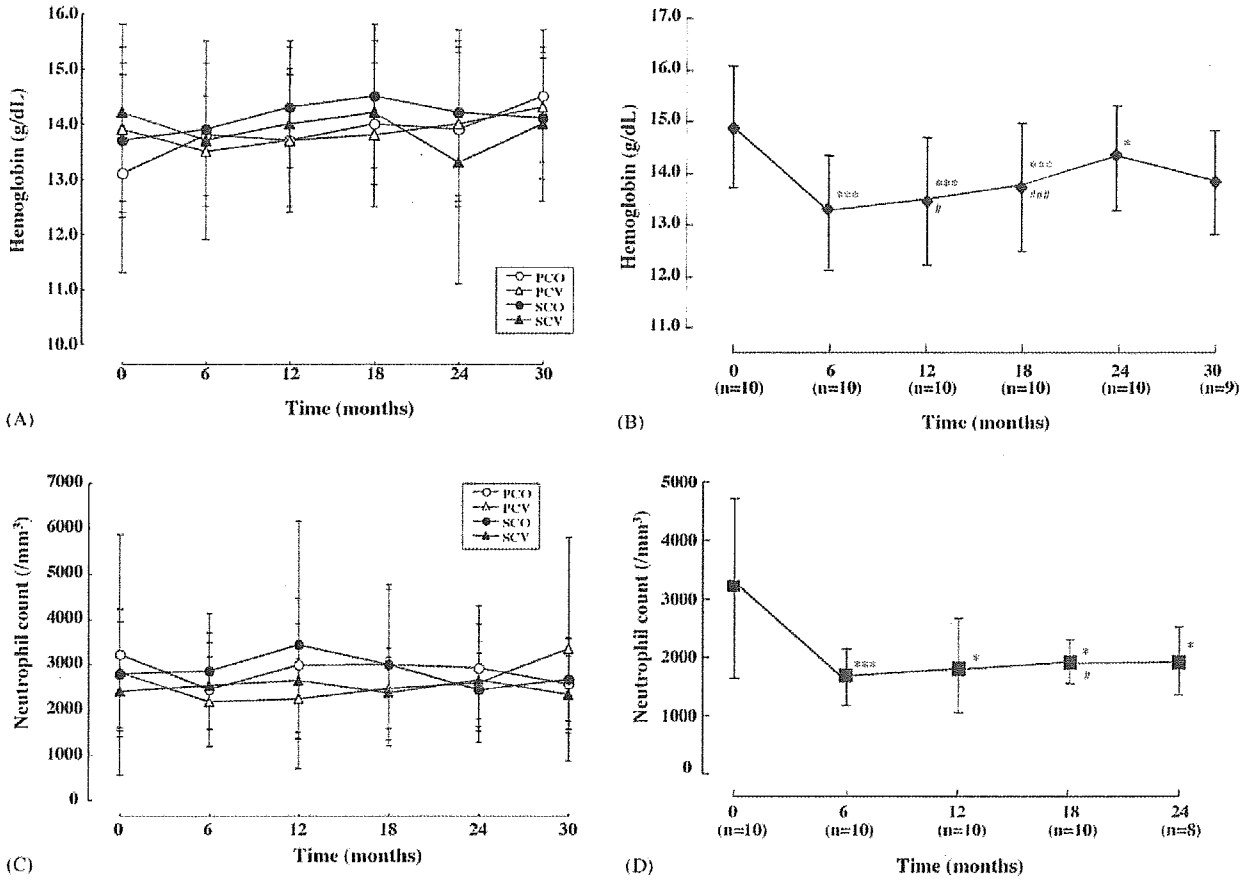

Fig. 1. Recovery after transient suppression of hemoglobin and neutrophil levels in patients with long-term use of Combivir. (A) Mean hemoglobin levels did not change significantly in all groups during each treatment. The baseline hemoglobin level in the Combivir group (PCV + SCV) was higher than in controls (PCO + SCO). (B) Mean hemoglobin levels at 6, 12, 18 and 24 months after start of treatment decreased significantly compared to baseline in the subgroup A of PCV group ($n = 10$). However the decreased hemoglobin level gradually reverted to the baseline levels despite continuation of the same regimen. Hemoglobin levels at 12 and 18 months were significantly high compared to findings at 6 months. (Wilcoxon matched pairs signed rank test; $^{*,\#}p < 0.05$, $^{***,\#\#\#}p < 0.005$). (C) Mean neutrophil counts did not change significantly in all groups during each treatment. (D) Mean neutrophil counts at 6, 12, 18 and 24 months after beginning treatment decreased significantly compared to baseline in sub-group C of PCV group ($n = 10$). However, the neutrophil counts gradually reverted to baseline levels despite continuation of the same regimen. The neutrophil counts at 18 months was significantly high compared to that of 6 months (Wilcoxon matched pairs signed rank test; $^{*,\#}p < 0.05$, $^{***}p < 0.005$).

mary treatment groups such as PCV group and PCO group. It seems ZDV or d4T in the secondary treatment group affected red blood cell counts. However, after starting each treatment, MCV values increased and became high at around 110/mm^3 in all groups (Fig. 2A). Other laboratory test values did showed no notable changes (data not shown).

3.5. Adverse events

The most common adverse events in each group were nausea/vomiting, dizziness and malaise. Anemia was observed in two in the Combivir group and one in the control group. Discontinuing each treatment led to elimination of these adverse effects. The anemia in two in the Combivir group was observed 2 months after their starting treatment, and that in one in the control group was evident as early as the eighth day. The occurrence of anemia in the control group was on ZDV 400 mg/day + 3TC. The frequency of anemia in the Combivir group was 3.6% (2/55) and similar to that in the control group {2.6% (1/39)}. The 20 in the control group on ZDV + 3TC regimen were on a ZDV 400 mg/day. We compared the safety profile of ZDV 600 mg/day to ZDV 400 mg/day. Adverse events rate of Combivir was 50.9% (28/55) and 60.0% (12/20) of AZT + 3TC group. Moreover, the number who discontinued Combivir group was 7 (12.7%) and that in ZDV + 3TC group was 5 (25.0%). In the SCV group, nineteen were changed to Combivir from ZDV 400 mg/day + 3TC. There were six with some adverse events and these were similar to other groups' events. These observations suggest that increasing the ZDV dose to 600 mg/day does not affect the incidence of adverse events. In addition there were no concomitantly used drugs that could affect pharmacokinetic parameters of ZDV and enhance its toxicity.

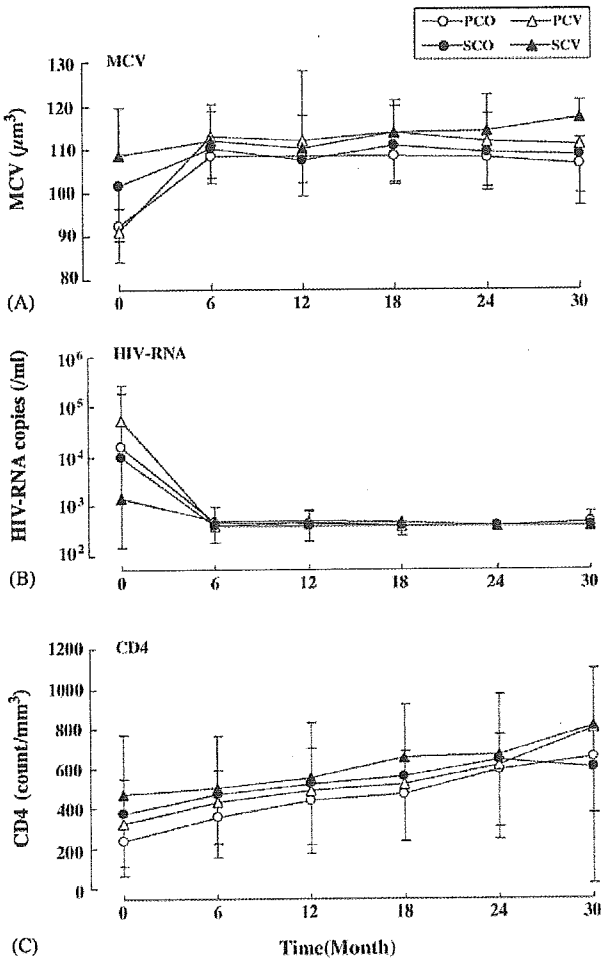

Fig. 2. Changes in MCV values, HIV RNA level and CD4$^+$ T cell counts in each group of patients. (A) MCV values for the secondary treatment group such as SCV and SCO group were higher than for primary treatment groups such as PCV and PCO group at baseline. However, after starting each treatment, MCV values increased and became high at around 110/mm^3 in all groups. (B) Mean HIV RNA level in all groups of treatment decreased compared to baseline significantly ($p<0.05$–$p<0.001$; Wilcoxon matched pairs signed rank test). (C) Mean CD4$^+$ T cell counts in all groups of treatment increased significantly compared to the baseline ($p<0.05$–$p<0.001$; Wilcoxon matched pairs signed rank test).

3.6. Effects on viral load and CD4$^+$ T-cell counts

Baseline viral load in the primary treatment group (PCV + PCO) was higher than in the secondary treatment group (SCV + SCO). Mean baseline viral loads of each group were $10^{4.6}$ copies/mL (PCV), $10^{4.0}$ copies/mL (PCO), $10^{3.0}$ copies/mL (SCV) and $10^{3.7}$ copies/mL (SCO), respectively. However, after starting each treatment, HIV RNA was not detectable in serum samples from in each group (VL < 50 or <400 copies/mL) (Fig. 2B). Baseline CD4$^+$ T-cell count in the SCV group was 518/mm^3 and higher than other groups (PCV: 304/mm^3, SCO: 345/mm^3, PCO: 277/mm^3) significantly ($p<0.001$; Student's t-test) (Fig. 2C). This result suggests effective treatment with the previous combination for the SCV group. CD4$^+$ T-cell counts during each treatment increased significantly ($p<0.05$–$p<0.001$; Wilcoxon matched pairs signed rank test) and reached over 600/mm^3 at 30 months in all groups (Fig. 2C).

4. Discussion

The nucleoside reverse transcriptase inhibitor (NRTI) was first developed as an anti-HIV drug. However, the appropriate dosage was unclear because this type of drug is only active after being phosphorylated inside cells. A daily dose of 400 mg of ZDV has been widely used in Japan because anemia and neutropenia occurred frequently in cases of ingesting a higher dose (800 mg/day) than did 400 mg/day of ZDV in a clinical trial conducted in Japan (Kimura et al., 1992). Bone marrow toxicity associated with AZT such as macrocytic anemia and neutropenia has been frequently reported for the patients treated with a higher dose of ZDV mono therapy (Richman et al., 1987). Given the dose-dependent nature of these adverse effects, Japanese health care providers have some hesitance to prescribe Combivir that contains 600 mg of ZDV, as the daily dose. Data on four patients with severe anemia associated with Combivir have also been reported (Sibery et al., 2003). To evaluate the long-term toxicity of Combivir, we reviewed clinical records of HIV-1 infected Japanese patients on treatment with Combivir-containing regimen.

The results in this retrospective study showed that anemia and adverse events occurred at comparable frequency in each group of patients. Consistent with previous reports (Hester and Peacock, 1998; Tseng et al., 1998) these adverse events occurred in less than a few months after starting each treatment. The frequency of anemia in the Combivir group was only 3.7% (2/54), and it was similar to that for ZDV 400 mg/day + 3TC group (5.0%) group. In other words there was no difference in these groups with respect to the frequency of anemia by the difference in the dose of ZDV. It is also of note that the efficacy of Combivir was comparable to that of 400 mg of ZDV of four times a day with a twice a day dosing of 3TC. However, we have to take into account the fact that Combivir was prescribed for heavy weight patients. And such may mask the occurrence of adverse events as well as the difference in efficacy.

We observed a certain degree of decrease in hemoglobin levels and neutrophil counts in the subgroups of patients in PCV (subgroups A and C, respectively). Interestingly, a gradual recovery of these hematological toxicities occurred despite the continuation of Combivir containing regimens. The mechanism whereby the risk of hematological toxicity associated with increasing ZDV dosages may be related to the intracellular accumulation of the toxic metabolite zidovudine monophosphate (AZTMP) (Tornevik et al., 1995). AZTMP interferes with both cellular DNA synthesis and exonuclease-catalyzed removal of ZDV from host cell DNA (Sommadossi et al., 1989; Harrington et al., 1993). In addition, at clinically

relevant concentrations, AZTMP acts as a potent inhibitor of the transport of pyrimidine nucleotide sugars into the Golgi complex, thereby inhibiting protein glycosylation and altering glycosphingolipid synthesis (Yan et al., 1995). Therefore, AZTMP may elicit cytotoxic effects on rapidly growing erythrocytes and neutrophil precursors, both by interfering with nuclear DNA replication and by compromising the function of membrane receptors involved in receiving of extracellular stimuli required for cell growth and differentiation. From these observations it seems reasonable to speculate that either decrease in the intracellular concentration of AZTMP or compensatory mechanisms that improve the signal transduction for erythropoiesis and myelopoiesis mediated by cytokines contributed the recovery from hematological toxicities.

Two mechanisms may be related to the decrease in the concentration of AZTMP: altered metabolism of nucleoside analogues due to impaired nucleoside phosphorylation and increased efflux of the compounds by membrane transport mechanisms (Schuetz et al., 1999; Wijnholds et al., 2000). These mechanisms have been considered to contribute to the cellular drug-resistance (Dianzani et al., 1994; Groschel et al., 1997; Fridland et al., 2000; Turriziani et al., 2000). However, there was no evidence of treatment failure for patients in our PCV group as we found an increase in $CD4^+$ cell counts and an undetectable HIV-RNA load. Furthermore, the MCV level which is associated with the intracellular increase of AZTMP was kept high. These observations suggest that decrease in the level of AZTMP in the course of long-term treatment is unlikely although we must determine longitudinal changes of intracellular AZTMP level in precursors of blood cells in patients on Combivir treatment. Other compensatory mechanisms against the hematological toxicity may occur. An increase in erythropoietin or granulocyte-colony stimulating factor (G-CSF) levels in compensation for chronic anemia or neutropenia is another notion.

Acknowledgments

This work was supported in part by the Ministry of Health, Labor and Welfare of Japan (H-15-AIDS-001, -011, -015 and H-13-AIDS-001).

References

Dianzani F, Antonelli G, Turriziani O, Riva E, Simeoni E, Signoretti C, et al. Zidovudine induces the expression of cellular resistance affecting its antiviral activities. AIDS Res Hum Retroviruses 1994;10:1471–8.

Dieleman JP, Jambroes M, Gyssens IC, Sturkenboom MC, Stricker BH, Mulder WM, et al. Determinants of recurrent toxicity-driven switches of highly active antiretroviral therapy. The ATHENA Cohort. AIDS 2002;16:737–45.

Eron JJ, Yetzer ES, Ruane PJ, Becker S, Sawyerr GA, Fisher RL, et al. Efficacy, safety, and adherence with a twice-daily combination of lamivudine/zidovudine tablet formulation, plus a protease inhibitor, in HIV infection. AIDS 2000;14:671–81.

Fridland A, Connelly MC, Robbins BL. Cellular factors for resistance against antiretroviral agents. Antiviral Ther 2000;5:181–5.

Groschel B, Cinatl J, Cinatl Jr J. Viral and cellular factors for resistance against antiretroviral agents. Intervirology 1997;14:400–7.

Harrington JA, Reardon JE, Spector T. 3′-Azido-3′-deoxythymidine (AZT) monophosphate: an inhibitor of exonucleolytic repair of AZT terminated DNA. Antimicrob Agents Chemother 1993;37: 918–20.

Hester EK, Peacock Jr JE. Profound and unanticipated anemia with lamivudine-zidovudine combination therapy in zidovudine-experienced patients with HIV infection. AIDS 1998;12:439–40.

Kimura S, Oka S, Toyoshima T, Hirabayashi Y, Kikuchi Y, Mitamura K, et al. A randomized trial of reduced doses of azidothymidine in Japanese patients with human immunodefiency virus type 1 infection. Intern Med 1992;31:871–6.

Kimura S, Yamada K, Ito A, Mimaya J, Takamatsu J, 3TC Study Group. Phase 2 clinical study on 3TC (Lamivudine) in HIV infections. Antibiot Chemother 1998;14:1419–32.

Moses A, Nelson J, Bagby Jr GC. Review article: the influence of human immunodeficiency virus-1 on hematopoiesis. Blood 1998;91:1479–95.

Richman DD, Fischl MA, Grieco MH, Gottlieb MS, Volberding PA, Laskin OL, et al. The toxicity of azidothymidine (AZT) in the treatment of patients with AIDS and AIDS-related complex. A double-blind, placebo-controlled trial. N Engl J Med 1987;317:192–7.

Schuetz JD, Connelly MC, Sun D, Paibir SG, Flynn PM, Srinivas RV, et al. MRP4: a previously unidentified factor in resistance to nucleoside-based antiviral drugs. Nat Med 1999;5:1048–51.

Sibery MJ, Astrow A, Kempin S, Halperin I. Combivir (AZT/3TC) therapy is associated with life-threatening anemia in patients with HIV infection. Blood 2003;102:51b (Abstract 3907).

Sommadossi JP, Carlisle R, Zhou Z. Cellular pharmacology of 3-azido-3′-deoxythymidine with evidence of incorporation into DNA of human bone marrow cells. Mol Pharmacol 1989;36:9–14.

Tornevik Y, Ullman B, Balzarini J, Wahren B, Eriksson S. Cytotoxicity of 3′-azido-3′-deoxythymidine correlates with 3′-azidothymidine-5′-monophosphate (AZTMP) levels, whereas anti-human immunodeficiency virus (HIV) activity correlates with 3′-azidothymidine-5′-triphosphate (AZTTP) levels in cultured CEM T-lymphoblastoid cells. Biochem Pharmacol 1995;49:829–37.

Tseng A, Conly J, Fletcher D, Keystone D, Salit I, Walmsley S. Precipitous declines in hemoglobin levels associated with combination zidovudine and lamivudine therapy. Clin Infect Dis 1998;27:908–9.

Turriziani O, Antonelli G, Dianzani F. Cellular factors involved in the induction of resistance of HIV to antiretroviral agents. Int J Antimicrob Agents 2000;16:353–6.

Wijnholds J, Mol CA, van Deemter L, de Haas M, Scheper GL, Baas F, et al. Multidrug-resistance protein 5 is a multispecific organic anion transporter able to transport nucleotide analogs. Proc Natl Acad Sci USA 2000;97:7476–81.

Wilde MI, Langtry HD. Zidovudine. An update of its pharmacodynamic and pharmacokinetic properties, and therapeutic efficacy. Drugs 1993;46:515–78.

Yan JP, Ilsley DD, Frohlick C, et al. 3′-Azidothymidin (zidovudine) inhibits glycosylation and dramatically alters glycosphingolipid synthesis in whole cells at clinically relevant concentrations. J Biol Chem 1995;270:22836–41.

Yeni PG, Hammer SM, Carpenter CCJ, Cooper DA, Fischl MA, Gatell JM, et al. Antiretroviral treatment for adult HIV infection. 2002. Updated recommendation of the International AIDS Society-USA Panel. JAMA 2002;288:222–35.

ELSEVIER

Neurobiology of Disease

www.elsevier.com/locate/ynbdi
Neurobiology of Disease 20 (2005) 12–26

Increase of C1q biosynthesis in brain microglia and macrophages during lentivirus infection in the rhesus macaque is sensitive to antiretroviral treatment with 6-chloro-2′,3′-dideoxyguanosine

Candan Depboylu,[a,b] Martin K.-H. Schäfer,[a] Wilhelm J. Schwaeble,[a,c] Todd A. Reinhart,[d] Hitomi Maeda,[e] Hiroaki Mitsuya,[e] Ruslan Damadzic,[f] Dianne M. Rausch,[g] Lee E. Eiden,[f] and Eberhard Weihe[a,*]

[a]*Department of Molecular Neuroscience, Institute of Anatomy and Cell Biology, Philipps University, Robert-Koch-Str. 8, 35033 Marburg, Germany*
[b]*Department of Neurology, Center for Nervous Diseases, Philipps University, Marburg, Germany*
[c]*Department of Infection, Immunity and Inflammation, University of Leicester, Leicester, UK*
[d]*Department of Infectious Diseases and Microbiology, University of Pittsburgh, Pittsburgh, PA 15260, USA*
[e]*Division of Cancer Treatment, National Cancer Institute, NIH, Bethesda, MD 20892, USA*
[f]*Section on Molecular Neuroscience, Laboratory of Cellular and Molecular Regulation, National Institute of Mental Health, NIH, Bethesda, MD 20892, USA*
[g]*Division of Mental Disorders, Behavioral Research and AIDS, National Institute of Mental Health, NIH, Bethesda, MD 20892, USA*

Received 5 November 2004; revised 26 January 2005; accepted 31 January 2005
Available online 22 March 2005

Complement activation in the brain contributes to the pathology of neuroinflammatory and neurodegenerative diseases such as neuro-AIDS. Using semiquantitative in situ hybridization and immunohistochemistry, we observed an early and sustained increase in the expression of C1q, the initial recognition subcomponent of the classical complement cascade, in the CNS during simian immunodeficiency virus (SIV) infection of rhesus macaques. Cells of the microglial/macrophage lineage were the sources for C1q protein and transcripts. C1q expression was observed in proliferating and infiltrating cells in SIV-encephalitic brains. All SIV-positive cells were also C1q-positive. Treatment with the CNS-permeant antiretroviral agent 6-chloro-2′,3′-dideoxyguanosine decreased C1q synthesis along with SIV burden and focal inflammatory reactions in the brains of AIDS-symptomatic monkeys. Thus, activation of the classical complement arm of innate immunity is an early event in neuro-AIDS and a possible target for intervention.

Keywords: Complement; Microglia; Neuro-AIDS; Antiretroviral treatment; Blood–brain barrier; Cell proliferation

Introduction

The complement system is a major component of the innate immune system. It is composed of more than thirty soluble and membrane-anchored proteins. Three possible complement activation cascades generate opsonins, inflammatory mediators, and cytolytic protein complexes which play an important role in clearing microorganisms and tissue damage products (Whaley and Schwaeble, 1997). Locally synthesized complement components and regulators are present at higher than normal levels in a variety of human and animal neurodegenerative (Farkas et al., 2003; Kovacs et al., 2004; Rostagno et al., 2002; Schäfer et al., 2000; Singhrao et al., 1996; Velazquez et al., 1997; Yamada et al., 1994) and neuroinflammatory diseases (Dietzschold et al., 1995; Walsh and Murray, 1998; Williams et al., 1994). Mice which are deficient in classical complement activation are partly protected against spongiform encephalopathy after intraperitoneal exposure to prion (Klein et al., 2001). On the other hand, complement activation can reduce neurodegeneration and plaque formation in a mouse model of Alzheimer's disease (Wyss-Coray et al., 2002).

Activation of complement was shown during the course of human immunodeficiency virus (HIV) infection in non-CNS tissues but little is known about the involvement of complement activation during HIV infection in the brain (Perricone et al., 1987; Senaldi et al., 1990). In vitro, complement activation may significantly enhance the infection of complement receptor-bearing cells by HIV-1 (Robinson et al., 1988, 1989, 1990; Sölder et al., 1989; Tremblay et al., 1990) or simian immunodeficiency virus (SIV) (Montefiori et al., 1990). Activation of the classical complement pathway in immunodeficiency virus infection may be through direct binding of C1q, the recognition subunit of the first complement component, to the retroviral glycoproteins

* Corresponding author. Fax: +49 6421 2868965.
E-mail address: weihe@staff.uni-marburg.de (E. Weihe).
Available online on ScienceDirect (www.sciencedirect.com).

0969-9961/$ - see front matter © 2005 Elsevier Inc. All rights reserved.
doi:10.1016/j.nbd.2005.01.030

gp41 or *gp120* (Ebenbichler et al., 1991), or as a result of interaction of C1q with immune complexes of envelope-specific antibodies.

The aims of this study were to investigate whether C1q is produced locally in the brain in the course of lentiviral infection, to identify the cell types responsible for the biosynthesis of C1q peptide chains, and to characterize the regulation of C1q expression through the disease process and therapeutic intervention. We used a well-established primate model for human HIV infection–SIV infection of rhesus macaques. Like HIV-infected individuals, rhesus monkeys infected with SIV develop acquired immunodeficiency syndrome (AIDS) and neurological complications including cognitive and motor deficits (Murray et al., 1992). Impairments occur with low or marked encephalitis with the appearance of astrogliosis, nodule and giant cell formation, inflammatory infiltrates, myelin pallor, and vessel leakage (Budka, 1986; Lane et al., 1996; Luabeya et al., 2000; Weihe et al., 1993). Loss of synapses, dendrites, and neurons also occurs in SIV disease (Bissel et al., 2002; Li et al., 1999; Luthert et al., 1995). Neurodegenerative damage is thought to be related to SIV replication, the number of inflammatory cells infiltrating and activated in the brain, and the amount of host- and/or virus-derived cytotoxins produced (Bissel et al., 2002; Glass et al., 1995; Li et al., 1999; Lipton et al., 1991; Power et al., 2002).

In order to understand the effect of CNS-permeant antiretroviral treatment on neurochemical sequelae during simian AIDS, we explored additionally the effects of the lipophilic antiretroviral agent 6-chloro-2′,3′-dideoxyguanosine (6-Cl-ddG) on C1q expression. 6-Cl-ddG is a congener of 2′,3′-dideoxyguanosine and penetrates efficiently into the CNS in monkeys (Hawkins et al., 1995). It is highly active against HIV-1 and SIV in vitro (Fujii et al., 1998; Shirasaka et al., 1990), and in vivo (Depboylu et al., 2004; Fujii et al., 1997a,b, 1998). Our data demonstrate a relationship between C1q expression and virus burden, as well as disease progression and CNS-directed antiretroviral therapy during lentiviral infection of the brain.

Materials and methods

Virus stock, inoculation procedures in rhesus monkeys, and antiretroviral treatment

Juvenile rhesus macaques, which were determined negative for simian retrovirus-1 and -2, simian immunodeficiency virus, and simian herpes virus, were inoculated intravenously with ten rhesus infectious doses of cell-free SIV_{6B670} grown in human peripheral blood mononuclear cells. Virus was obtained as an aliquot of a previously characterized virus stock stored in liquid nitrogen (da Cunha et al., 1995). Following inoculation, animals were monitored and examined for clinical evidence of disease. Blood and cerebrospinal fluid (CSF) samples were obtained from the animals at regular intervals. Eight macaques exhibited clinical signs of acquired immunodeficiency syndrome (AIDS) and five did not at time of euthanasia (Depboylu et al., 2004). AIDS-defining criteria included one or more of the following: more than 10% loss of body weight, intractable diarrhea/dehydration requiring fluid replacement, oral lesions, and organ inflammations. Additionally, four SIV-infected monkeys, in which the viral load was found to be more than 100,000 virions/mL in plasma and more than 100 virions/mL in CSF in more than two consecutive examinations, underwent a treatment with 2′,3′-dideoxyinosine (ddI) or 6-chloro-2′,3′-dideoxyguanosine (6-Cl-ddG), and were euthanized shortly thereafter (see Depboylu et al., 2004). Three monkeys (MO76, MO77, and MO91) received 10 mg/kg/day ddI subcutaneously for 3 weeks for clinical stabilization and then 75 mg/kg/day of 6-Cl-ddG subcutanously for 6 weeks. A fourth monkey (MO89) received only 6-Cl-ddG (200 mg/kg/day) subcutaneously for 3 weeks. The vehicle for ddI administration was phosphate-buffered saline (PBS), and for 6-Cl-ddG administration, the vehicle was 70% propylene glycol/30% PBS. Four age-matched non-infected macaques were used as controls. Experiments involving the use of rhesus macaques were approved by the Animal Care and Use Committee of Bioqual, Inc., an NIH-approved and Association for Assessment and Accreditation of Laboratory Animal Care-accredited research facility. All experiments were carried out using the ethical guidelines promulgated in the National Institutes of Health Guide for the Care and Use of Laboratory Animals.

Tissue preparation for histochemical analysis

Prior to sacrifice, animals received ketamine (20 mg/kg) and were then anesthetized sequentially with ketamine–acepromazine (10 mg/kg) and perfused transcardially in the following sequence: 2 L/kg PBS, then 400 mL/kg of 1% formalin in PBS, followed by 1.5 L/kg of 4% formalin in PBS. Tissue specimens were obtained at necropsy and immersion-fixed overnight in 4% paraformaldehyde/PBS. Next, some blocks were cryopreserved in 10–20% sucrose in PBS and snap frozen in isopentane cooled to −70°C. Some blocks were postfixed in Bouin–Hollande solution (containing 4% picric acid, 2.5% cupric acetate, 3.7% formaldehyde, and 1% glacial acetic acid) or buffered formalin, followed by extensive washes in 70% 2-propanol, dehydration, and processing for paraffin embedding.

Generation of specific complementary RNA probes

Specific sense and antisense riboprobes were generated from linearized vector constructs by in vitro transcription using the appropriate RNA polymerases and [^{35}S]-UTP and digoxigenin-UTP as label. Vectors with inserts were pBluescript KS+ containing an ~0.65-kb fragment of human C1q A cDNA, pBluescript KS+ containing an ~0.4-kb fragment of human C1q B cDNA and pGEM-T easy containing an ~0.45-kb fragment of human C1q C cDNA, respectively (Sellar et al., 1991). To increase tissue penetration of probes, the generated cRNA transcripts were reduced to nucleotide fragments of approximately 200–250 nucleotides by limited alkaline hydrolysis. The specificity of in situ hybridization signals was assessed by performing experiments with cRNA probes in sense strand orientation on subjacent sections.

Radioactive and non-radioactive in situ hybridization (ISH) histochemistry

ISH was performed according to the protocol reported by Schäfer et al. (1992) with some modifications (Depboylu et al., 2004). Frozen sections (14 μm) were cut from cryopreserved tissues, and thaw-mounted on superfrost plus microscope slides. Alternatively, paraffin embedded formalin-fixed brain tissue

sections (10 μm) were cut, deparaffinized in xylene, and rehydrated through graded series of 2-propanol. For pretreatment, sections were boiled in 10 mM sodium citrate buffer (pH 6.0) at 95°C for 15 min, washed in 10 mM PBS and in 0.4% Triton X-100/PBS. After rinsing in distilled water, sections were acetylated with triethanolamine/acetic anhydride (pH 8.0) for 10 min at room temperature (RT), followed by a wash in distilled water, and then dehydrated in graded ethanols, air dried, and directly used for hybridization, or stored at −20°C until use.

For radioactive hybridization, sections were incubated with cRNA probes diluted in hybridization buffer {50% formamide, 10% dextran sulfate, 3× saline sodium citrate (SSC), 50 mM sodium phosphate (pH 7.4), 10 mM dithiothreitol (DTT), 1× Denhardt's solution [0.02% Ficoll 400, 0.02% polyvinylpyrrolidone, 0.02% bovine serum albumine (BSA)], 0.1 mg/mL yeast tRNA} to a final concentration of 50×10^3 dpm/μL. DTT was added to a final concentration of 10 mM. 20- to 30-μL hybridization mix was applied and slides were coverslipped. Hybridization was carried out at 60°C in a humid chamber. After 16 h, coverslips were removed in 2× SSC at RT and the sections washed in the following order: 20 min in 1× SSC, 30 min RNAse buffer (10 mM Tris, pH 8.0, 0.5 M NaCl and 1.0 mM EDTA; containing 20 μg/mL RNAse A and 1 U/mL RNAse T1) at 37°C, in 1×, in 0.5×, and in 0.2× SSC each for 20 min, 60 min in 0.2× SSC at 60°C, and 10 min in 0.2× SSC and 5 min in distilled water at RT. The tissue was then dehydrated in graded ethanols and air dried. For visualization of hybridization signals, sections were coated with nitroblue tetrazolium (NBT)-2 nuclear emulsion (Eastman Kodak, Rochester, NY) and stored at 4°C. After 2–3 weeks of exposure, slides were developed (Kodak D19), fixed, counterstained with hematoxylin, dehydrated through graded series of ethanol, and coverslipped.

For non-radioactive detection, riboprobes were generated by in vitro transcription with a digoxigenin labeling mix containing 10 mM each of ATP, CTP, and GTP, 6.5 mM UTP, and 3.5 mM digoxigenin-11-UTP (Boehringer, Germany). After hydrolysis, probes were purified by sodium acetate precipitation and added in hybridization buffer to a final concentration of 1 ng/μL. Hybridization and washing procedures were performed as described above for radioactive detection. For the detection of non-radioactive hybrids, slides were equilibrated to buffer 1 (100 mM Tris and 150 mM sodium chloride, pH 7.5) containing 0.05% Tween 20 (Merck, Germany). Blocking was performed by incubation for 1 h in blocking buffer (buffer 1 containing 2% normal lamb serum). Alkaline phosphatase-conjugated anti-digoxigenin Fab fragments (Boehringer, Germany) were diluted to 1 U/mL in blocking buffer. After the slides were rinsed with buffer 1, the diluted antibody was applied for 1 h at RT. After washes in buffer 1, slides were equilibrated to buffer 2 (100 mM Tris, 100 mM sodium chloride, and 50 mM magnesium chloride, pH 9.4) containing 0.05% Tween 20 before a 72-h color reaction in buffer 2 containing 0.2 mM 5-bromo-4-chloro-3-indolyl phosphate (BCIP) and 0.2 mM NBT-2 salt (Boehringer, Germany) at 4°C. The reaction was stopped by washing the slides in distilled water, counterstained with hematoxylin, and coverslipped.

Hybridized sections were analyzed in dark or bright field illumination and photographed with the Olympus AX70 microscope (Olympus Optical, Germany).

Single enzymatic and single fluorescence immunohistochemistry (IHC)

A previously reported protocol for IHC was used with some modifications (Rohrenbeck et al., 1999; Schäfer et al., 2000). Deparaffinized paraffin-embedded tissue sections (7 μm) or cryosections (14 μm) were rehydrated through graded series of 2-propanol, incubated in methanol/H_2O_2 for 30 min, and boiled in 10 mM sodium citrate buffer (pH 6.0) at 95°C for 15 min. After several rinses in 50 mM PBS, sections were incubated in PBS containing 5% BSA for 30 min and in 1% BSA/PBS for 15 min. Thereafter sections were incubated with 30% avidin-blocking kit in 1% BSA/PBS and 30% biotin-blocking kit in 1% BSA/PBS (Vectastain Elite Avidin–Biotin-Blocking kit, Boehringer, Germany) for 15 min at RT. Then, primary antibodies were applied. A sheep polyclonal antibody against C1q protein (ICN Biochemicals, CA) which did not differentiate between the C1q A, B, and C chains was used at a 1:15,000 dilution. The proliferation marker Ki67 was detected with the mouse monoclonal antibody MIB-1 (Dianova, Germany) at a 1:200 dilution. Cells of mononuclear origin and endothelial cells were visualized with the biotinylated isolectin RCA-120 (Dianova, Germany) at a 1:5000 dilution. The primary antibodies were applied in 1% BSA/PBS and incubated at 16°C overnight followed by 2 h at 37°C and 2 h 27°C. After several washes in distilled water followed by rinsing in PBS, sections were incubated with species-specific biotinylated secondary antibodies (Dianova, Germany) for 1 h at 37°C, washed several times and incubated for 45 min with avidin–biotin–peroxidase complex reagents (Vectastain Elite ABC kit, Boehringer, Germany). Immunoreactions were visualized with 3,3′-diaminobenzidine (DAB, Sigma, Germany), resulting in a brown staining, or enhanced by the addition of 0.08% ammonium nickel sulfate (Fluka, Buchs, Switzerland), resulting in a dark blue staining. After three 5-min washes in distilled water, the sections were dehydrated through graded series of 2-propanol and coverslipped.

For immunofluorescence, C1q was detected with the sheep polyclonal antibody (ICN Biochemicals, CA) at a 1:1000 dilution. In addition, the following antibodies against brain resident cell markers were used. The mouse monoclonal antibody KP1 (DAKO, Denmark) recognized the macrophage activation marker molecule CD-68 and was used at a 1:50 dilution. Endothelial cells were visualized with a rabbit polyclonal antibody against von Willebrand factor (vWF; DAKO, Germany) at a 1:400 dilution. The biotinylated isolectin *ricinus communis* agglutinin-120 (RCA-120; Dianova, Germany) detected the cells of mononuclear origin and the endothelial cells (1:500 diluted). Neurons were visualized with a mouse monoclonal antibody recognizing the neuronal marker antigen NeuN (MAB377; Chemicon, Temecula, CA) at a 1:300 dilution. Astrocytes were stained with a polyclonal antibody from guinea pig against glial fibrillary acid protein (GFAP; 1:400 diluted; Progen, Germany). Oligodendrocytes were identified with a mouse monoclonal antibody Ab-1 recognizing 2′,3′-cyclic nucleotide-3′-phosphodiesterase (CNPase; Neomarkers, Fremont, USA) at a 1:50 dilution. Proliferating cells were visualized with the mouse monoclonal antibody MIB-1 against Ki67 (1:50 diluted). Immunoreactions were visualized by incubation with either species-specific indocarbocyamine-conjugated IgG (Cy3; Dianova, Germany), resulting in red–orange fluorescence labeling, or with species-specific biotinylated IgG (Dianova, Germany) both diluted 1:100 in 1% BSA/PBS for 1 h at 37°C and then, after a 15-min

wash in PBS, with Alexa 488-conjugated streptavidin (MoBiTec, Germany) at a 1:200 dilution in 1% BSA/PBS for 2 h at 37°C, resulting in green fluorescence. The biotinylated isolectin RCA-120 was visualized with Alexa 488-conjugated streptavidin. After extensive washes in distilled water, sections were further processed or coverslipped.

Fluorescence signals were analyzed and photographed with the Olympus AX70 microscope (Olympus Optical, Germany) or with the Olympus Fluoview confocal laser scanning microscope (Olympus Optical, Germany).

Double enzymatic and double fluorescence IHC

To visualize two different antigens in the same section, double IHC was carried out with primary antibodies from different species. The proliferation marker Ki67 was detected with nickel-enhanced DAB-visualization resulting in a nuclear dark blue staining. Prior to application of the antibody against C1q, the avidin–biotin–peroxidase from the first visualization procedure was blocked by incubation of sections in methanol/H_2O_2 and in avidin–biotin-blocking kit. C1q-immunoreactivity was visualized as described above but without nickel enhancement resulting in a cytoplasmic brown reaction product. To identify cell types immunopositive for C1q, double immunofluorescence for C1q and for the appropriate markers for brain resident cells (see above) was carried out. Sections were analyzed by high-power confocal laser scanning microscopy.

Double ISH histochemistry

Detection of two different RNA transcripts in the same tissue section was performed with radioactive and non-radioactive labeled riboprobes as described previously (Schäfer and Day, 1994). Digoxigenin-labeled and [^{35}S]-labeled probes were diluted in the same hybridization buffer in working concentrations. Hybridization and post-hybridization were carried out as described above. Non-radioactive signals were detected first. For the detection of radioactive-labeled probes, slides were air dried and covered with K5 photoemulsion (Ilford, England) diluted 1:1 in distilled water and stored at 4°C. Exposure times were 2–4 weeks.

Immunofluorescence combined with ISH histochemistry

For visualizing of an antigen with an RNA transcript in the same tissue section, IHC was performed in combination with ISH. Prehybridization, hybridization with the [^{35}S]-labeled probe against C1q A mRNA, and post-hybridization were performed. Before covering the slides with K5 photoemulsion (Ilford, England) for a 3-week exposure at 4°C, C1q or RCA-120 immunofluorescence staining was performed.

Detection of viral burden

Viral transcription and translation were detected by ISH and IHC. The monoclonal antibody KK41 against the SIV_{mac251} envelope glycoprotein *gp41* (NIH AIDS Research and Reference Program, Bethesda, MD, USA) was used to detect the crossreacting SIV_{SBG670} *gp41* (Kent et al., 1992). Single enzymatic (KK41 diluted 1:2000) and immunofluorescence (KK41 diluted 1:200) detection of *gp41* were carried out as described above. To assess the relationship of C1q with viral *gp41*, sections were co-stained for C1q and *gp41* double immunofluorescence as described above. ISH was performed using probes generated by incorporation of [^{35}S] into SIV RNA probes by in vitro transcription of SIV_{mac239} sequences cloned in a $pTRIK_{AN}19$ vector, or into DNA probes by random priming using sequences of cloned $SIV_{macBK28}$ DNA (Depboylu et al., 2004; Reinhart et al., 1997). Activities of radioactive probes were 30–50 × 10^3 dpm/μL. The DNA templates were a *Kpn*I fragment from the *pol* gene of SIV_{mac239} (nucleotide positions 5208–4713) or a *Bam*HI fragment from $SIV_{macBK28}$ (nucleotide positions 1841–9174). In some experiments, in situ hybridization experiments were performed with oligonucleotides specific for unspliced SIV RNA complementary to sequences at the exon/intron junction at the 5′-end of unspliced RNA (nucleotide positions 996–967 of SIV_{smH4} proviral sequence) as described by Reinhart et al. (1997). The sequences in the control sense probe were identical to sequences at the same exon/intron junction (nucleotide positions 967–996 of SIV_{smH4}). Polyacrylamide gel purified nucleotides were 3′-end-labeled with [^{35}S]-dCTP using terminal deoxynucleotide transferase to specific activities of 2–8 × 10^9 cpm/μg. For ISH, slide-mounted sections (14 μm) of cryopreserved tissues were postfixed in 4% paraformaldehyde/PBS, washed, and dehydrated. Pretreatments consisted of incubation for 20 min each in 0.2 N HCl at ambient temperature; 2× SSC at 70°C; and 2 mM $CaCl_2$, 20 mM Tris (pH 7.5), and 10 μg/mL proteinase K at 37°C, followed by washing, acetylation, and dehydration. Sections were then hybridized for 18 h at 45°C (for riboprobes) or at 37°C (for oligonucleotide probes). After post-hybridization, sections were coated with NTB-2 emulsion and exposed at 4°C for 3–6 days. After development, the sections were counterstained with cresyl violet.

Quantification of C1q A mRNA-positive cells

The average number of C1q A mRNA-positive cells was determined by cell counts in at least 15 random areas (each 0.1 mm^2) per section of striatum and insular cortex in a magnification which allowed the discrimination of cellular features. Three to eight interval sections of striatum and insular cortex were analyzed per animal. Cells with a nucleus were accepted as positive when having greater number of silver grains over their cytoplasm than background. Each multinucleated giant cell and cluster of cells, where the individual cell borders could not be distinguished, were counted as single cells. Quantitative image analysis was performed with the MCID M4 image analysis system (Imaging Research, St. Catharines, ON, Canada). Data were expressed as mean number (±SEM) of positive cells per 0.1 mm^2 area per experimental group.

Quantification of silver grains per C1q A mRNA-positive cell

After radioactive ISH, the number of silver grains per C1q A mRNA-positive cell in striatum and insular cortex were counted under highest magnification. Three to eight interval sections of striatum and insular cortex per monkey were analyzed. At least 20 random cells per section of striatum and insular cortex were analyzed by computer-assisted image analysis (MCID M4 image analysis system, Imaging Research, St. Catharines, ON, Canada). Multinucleated giant cells and clusters of cells, where the cell

borders could not be distinguished, were not included for the counting. From the average grain number per cell of the section labeled with the antisense probe for C1q A mRNA, the average background grain number per cell of the subjacent section labeled with the sense probe for C1q A mRNA was subtracted to get the net grain number per cell. Data were expressed as mean number (±SEM) of grains per C1q A mRNA-positive cell per experimental group.

Quantification of cells immunopositive for C1q and/or the proliferation marker Ki67

Three to eight interval sections per area and per monkey with double IHC for C1q and Ki67 were analyzed at a magnification which allowed the discrimination of cellular features. Immunopositive cells with a nucleus were counted in more than four random 0.1 mm^2 areas per section of insular, occipital, and basofrontal cortices, striatum, and corpus callosum. Dark blue cell nuclei stained for Ki67 and cells stained brown for C1q were counted. Then, the cells co-stained for C1q and Ki67 were counted. In animals exhibiting AIDS (SIV,+AIDS and SIV,+AIDS,+ddG), the number of C1q- and/or Ki67-positive cells, which were parenchymal, intravascular, and perivascular, were counted separately. For total number of cells, all three were summed. Each multinucleated giant cell and cluster of cells, where the individual cell borders could not be distinguished, were counted as single cells having one nucleus. Quantitative image analysis was performed with the MCID M4 image analysis system (Imaging Research, St. Catharines, ON, Canada). Data were expressed as mean number (±SEM) of cell per 0.1 mm^2 area per experimental group.

Statistics

One-way non-parametric analysis of variance (ANOVA) and the post hoc Newman–Keuls Multiple Comparison Test were used to evaluate statistical differences between the experimental groups. Unpaired, two-tailed Student's t test was assessed when comparing antiretroviral untreated and treated AIDS-diseased animal groups. Values of P less than 0.05 were considered statistically significant.

Results

Brain tissue sections of non-infected control monkeys (Ctrl), SIV-infected monkeys without AIDS (SIV,−AIDS), and SIV-infected monkeys exhibiting AIDS (SIV,+AIDS) were analyzed. A fourth group consisted of monkeys with high viremia and increased viral load in CSF at initiation of antiretroviral treatment and suffering from AIDS (SIV,+AIDS,+ddG). All animals are summarized in Table 1.

Table 1
Infection duration, treatment regime, brain virus burden, and signs of encephalitis in monkeys at time of euthanasia and necropsy

Monkey number	Duration of infection (months)	Drug treatment	Brain SIV burden[c]	Degree of SIV-induced encephalitis[d]	Clinical findings
44	Not infected	Not treated	−	−	No disease
50	Not infected	Not treated	−	−	No disease
69	Not infected	Not treated	−	−	No disease
87	Not infected	Not treated	−	−	No disease
75	2.5	Not treated	−	−	Asymptomatic
80	6.5	Not treated	−	−	Asymptomatic
85	4.5	Not treated	−	−	Asymptomatic
92	6.0	Not treated	−	−	Asymptomatic
93	4.5	Not treated	−	−	Asymptomatic
46	19.0	Not treated	+	+	Diarrhea, mycotic infection, mass
71	6.5	Not treated	++	++	Diarrhea, listless, rash
74	6.0	Not treated	+++	+++	Diarrhea, anemia, parasitic infection, LN atrophy
78	2.4	Not treated	+++	+++	Diarrhea, parasitic infection, pneumonitis
79	2.5	Not treated	+	+	Rash, heart murmur, LN atrophy
82	3.0	Not treated	+++	+++	Diarrhea, wasting
86	4.5	Not treated	+++	+++	Wasting, mass, thrush, colitis, LN atrophy
90	2.3	Not treated	++	++	Vomiting, wasting, tube feed
76[a]	22.0	ddI/6-Cl-ddG	−	−	Wasting, diarrhea, heart murmur, anemia
77[a]	4.0	ddI/6-Cl-ddG	±	±	Incontinence, washing, diarrhea
89[b]	22.0	6-Cl-ddG	−	−	Anemia, wasting, diarrhea, lymphoma
91[a]	6.1	ddI/6-Cl-ddG	−	−	Wasting, diarrhea

6-Cl-ddG, 6-chloro-2′,3′-dideoxyguanosine; ddI, 2′,3′-diodeoxyinosine; LN, lymph node; SIV, simian immunodeficiency virus.

[a] Treatment with ddI prior with the CNS-permeant 6-Cl-ddG.

[b] Treatment only with 6-Cl-ddG.

[c] Detection of SIV *env/pol* by ISH; detection of SIV *gp41* by IHC. Scoring: −(ISH: no cells with more silver grains above background, defined as signal with the sense control probes and IHC: no immunoreactive cells) to +++ (ISH: >100 cells/mm^2 with intense collections of silver grains and IHC: >100 immunoreactive cells/mm^2); the numbers of cells/mm^2 were not specifically determined; sections from frontal, insular and occipital cortex, hippocampus, basal ganglia, thalamus, and brainstem were analyzed and summarized.

[d] SIV-induced mononuclear reactions monitored by IHC for RCA-120 or CD-68; scoring was as: +++ for severe, ++ for moderate, and + for mild SIV-induced encephalitis with appearance of macrophage nodules, mononuclear cell infiltrates, multinucleated giant cells, − for non-SIV-induced encephalitis.

Brain C1q protein and mRNA levels in early and late stage of SIV infection

Biosynthesis and regulation of C1q was examined at the transcriptional and translational level in the monkey central nervous system during SIV infection. IHC and ISH for C1q protein and mRNAs encoding the C1q peptide chains A, B, and C were carried out on brain tissue sections of non-infected control monkeys (Ctrl), SIV-infected monkeys without clinical symptoms of AIDS (SIV,−AIDS), and infected monkeys exhibiting AIDS (SIV,+AIDS). Immunohistochemistry for C1q revealed only few immunoreactive cells in cortical gray and white matter of non-infected monkeys as demonstrated for the insular cortex (Fig. 1A). SIV infection caused a moderate increase in the number of C1q-immunopositive cells and in the intensity of C1q cell immunoreactivity in insular cortex in early unproductive stage of disease (Fig. 1B). An even stronger increase in the number of C1q-immunostained cells was observed in late stage of disease with clinical manifestation of AIDS (Fig. 1C). Next, we explored whether the three C1q chains A, B, and C were co-upregulated, as

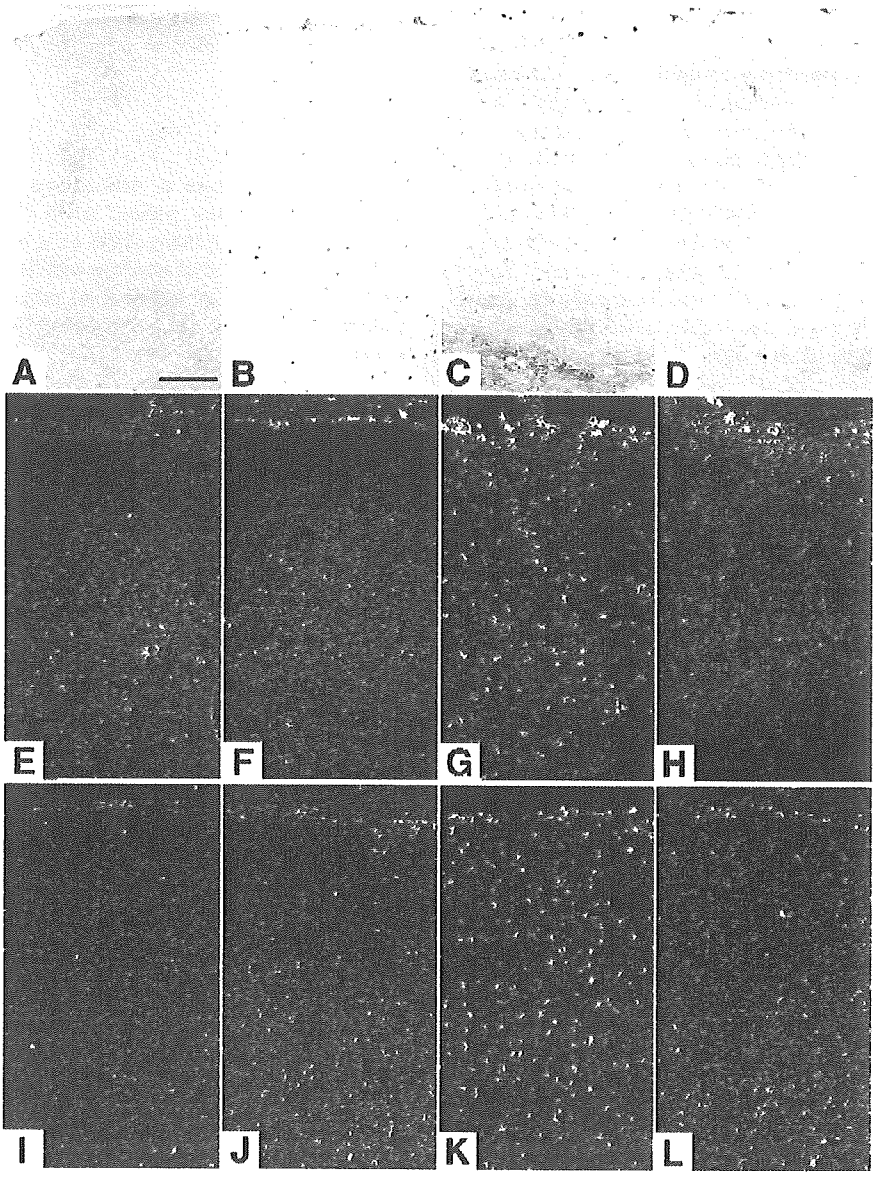

Fig. 1. Regulation of C1q protein and mRNA encoding C1q A and B chains in the rhesus monkey insular cortex in control (A, E and I), SIV infection without AIDS (B, F and J), SIV infection with AIDS (C, G and K) and SIV infection with AIDS and antiretroviral treatment (D, H and L). C1q-immunoreactivity is moderately increased in the insular cortex of monkeys without AIDS (B) and more strongly increased in monkeys exhibiting AIDS (C) as compared to non-infected control monkeys (A). After antiretroviral treatment of monkeys exhibiting AIDS, the number of C1q-immunoreactive cells is similar to that in early stages of disease (D). In situ hybridization signals for mRNA of C1q chains A and B are abundant in the insular cortex of monkeys with AIDS (G and K) as compared to control (E and I). After antiretroviral treatment, the number of cells demonstrating signals for C1q A and B mRNA (H and L) is similar to levels in the SIV,-AIDS group (F and J). Scale bar in A for A–L is 200 μm.

biologically active C1q protein requires the co-expression of all three C1q chains. The antibody we employed did not differentiate between the three C1q peptide chains; therefore, in situ hybridization was carried out to localize the three C1q transcripts.

In situ hybridization with [^{35}S]-labeled cRNA antisense probes demonstrated a similar pattern of changes in C1q A, B, C mRNA expression throughout all telencephalic lobes, hippocampus, striatum, and brainstem nuclei, indicating that bioactive C1q was produced. The changes of C1q mRNA expression in the four experimental groups are demonstrated for the C1q A and B chains (Figs. 1E–G and 1I–K). A marked increase in the density of cells expressing C1q A and B mRNAs was observed in the insular cortex of monkeys with AIDS. C1q mRNA was found to be copious in the cortex of SIV,+AIDS monkeys, and was distributed in a uniform, non-laminar pattern suggesting a non-neuronal localization. SIV-infected monkeys without AIDS exhibited only a moderate increase in cells expressing C1q mRNAs which occurred mainly in submeningeal spaces.

To quantify the observed changes of C1q mRNA and protein expression during SIV infection, cells stained for the C1q A chain mRNA shown to be representative for the B and C chains and C1q protein were counted. A dramatic increase in the number of cells expressing C1q A mRNA in the striatum and the insular cortex of monkeys with AIDS (43.9 ± 10.0 and 38.5 ± 7.5 cells per 0.1 mm^2 area) was observed (Table 2) as compared to the animals of the control (0.5 ± 0.1 and 0.4 ± 0.1 cells per 0.1 mm^2 area) or SIV,−AIDS groups (0.6 ± 0.4 and 0.5 ± 0.1 cells per 0.1 mm^2 area). Counting of C1q-immunopositive cells revealed an early upregulation of C1q protein biosynthesis during SIV infection before clinical symptoms became apparent (Table 2). In striatum and insular cortex of SIV,−AIDS animals, 7.9 ± 1.9 and 6.8 ± 3.7 cells per 0.1 mm^2 area, respectively, were detected as compared to control striatum and insular cortex (1.0 ± 0.2 and 2.3 ± 2.2 cells per 0.1 mm^2 area, respectively). In AIDS-diseased animals, even more C1q-immunoreactive cells were seen in the striatum (44.4 ± 7.5 cells per 0.1 mm^2 area) and in the insular cortex (40.6 ± 5.8 cells per 0.1 mm^2 area). Table 3 demonstrates additionally the number of C1q-immunopositive cells per area in occipital cortex, basofrontal cortex, and in corpus callosum of the Ctrl, SIV,−AIDS, and SIV,+AIDS groups. Grain counting revealed a significant ($P < 0.05$) increase in the C1q A mRNA abundance per cell in the brain of monkeys with AIDS as compared to non-infected monkeys and infected monkeys without AIDS (Table 2).

Table 2
Quantification of C1q protein-positive and C1q A mRNA-positive cells as well as of grains per C1q A mRNA-positive cell in the brain of rhesus macaques during SIV infection and antiretroviral treatment

Monkey groups	Insular cortex	Striatum
C1q protein-positive cells[a]		
Ctrl	2.3 ± 2.2	1.0 ± 0.2
SIV,−AIDS	6.8 ± 3.7	7.9 ± 1.9[c]
SIV,+AIDS	40.6 ± 5.8[b]	44.4 ± 7.5[b]
SIV,+AIDS,+ddG	6.8 ± 2.8	5.2 ± 2.0[c]
C1q A mRNA-positive cells[a]		
Ctrl	0.4 ± 0.1	0.5 ± 0.1
SIV,−AIDS	0.5 ± 0.1	0.6 ± 0.4
SIV,+AIDS	38.5 ± 7.5[b]	43.9 ± 10.0[b]
SIV,+AIDS,+ddG	9.3 ± 2.8[d]	9.2 ± 3.2[d]
Grains per C1q A mRNA-positive cell		
Ctrl	48.5 ± 9.1	41.1 ± 25.4
SIV,−AIDS	64.2 ± 10.7	62.2 ± 16.3
SIV,+AIDS	152.1 ± 22.6[b]	160.4 ± 24.5[b]
SIV,+AIDS,+ddG	82.0 ± 24.3	78.5 ± 24.3

ANOVA and the post hoc Newman–Keuls Multiple Comparison Test are used to evaluate statistical differences.

[a] Data expressed as mean number (±SEM) of C1q-positive cells per 0.1 mm^2 area.

[b] Statistically significantly different as compared to the other animal groups for the same brain area.

[c] Statistically significantly different only as compared to Ctrl group for the same brain area ($P < 0.05$).

[d] Statistically significantly different only as compared to Ctrl and SIV,−AIDS groups for the same brain area ($P < 0.05$).

Antiretroviral treatment and C1q protein and mRNA levels in the brain

To determine the impact of viral burden on the C1q biosynthesis in brain tissue, SIV-infected monkeys with high viremia and increased viral load in CSF were treated with 2′,3′-dideoxyinosine (ddI) for clinical stabilization followed by lipophilic 6-chloro-2′,3′-dideoxyguanosine (6-Cl-ddG). Only one animal (MO89) was treated only with 6-Cl-ddG. All animals receiving antiretroviral treatment with either ddI followed by 6-Cl-ddG or with 6-Cl-ddG alone exhibited clinical symptoms of AIDS (SIV,+AIDS,+ddG). In these four antiretrovirally treated animals, only minor upregulation of C1q was seen (Figs. 1D, H, and L) independently of whether they received combinatorial treatment or treatment with 6-Cl-ddG alone. This justifies analyzing these antiretrovirally treated animals as a group, though not homogeneous. Cell counting in striatum and insular cortex revealed that monkeys of the treated group had a higher density of cells expressing C1q A mRNA (9.2 ± 3.2 and 9.3 ± 2.8 cells per 0.1 mm^2 area, respectively) and C1q protein (5.2 ± 2.0 and 6.8 ± 2.8 cells per 0.1 mm^2 area, respectively) than monkeys of the Ctrl or SIV,−AIDS groups. Table 3 demonstrates additionally the density of C1q-immunopositive cells in occipital cortex, basofrontal cortex, and in corpus callosum of the SIV,+AIDS,+ddG group. As compared to non-treated AIDS-positive animals, all animals receiving antiretroviral treatment had a lower number of cells expressing C1q A mRNA and protein per area in the insular cortex and the striatum. The average grain number per C1q A mRNA-expressing cell was selectively increased in untreated symptomatic animals as compared to the other three groups (Table 2). Thus, antiretroviral treatment seemed to reduce C1q mRNA per cell in animals with AIDS.

Cellular expression of C1q protein and mRNA encoding C1q peptide chains A, B, and C

To identify the cell types producing C1q, high-power confocal laser scanning analysis was carried out after double immunofluorescence for C1q and the well-established microglia/macrophage activity marker CD-68, the astroglial marker GFAP, the oligodendroglial marker CNPase, the endothelial cell marker von Willebrand factor vWF, and the neuronal marker NeuN, respectively. C1q was co-localized with CD-68 in microglia/macrophages and multinucleated giant cells (Figs. 2A, B) but was absent from GFAP-positive astrocytes and CNPase-positive

Table 3
Proportional analysis of C1q-positive cells with Ki67-immunoreactivity in different brain regions during SIV infection and antiretroviral treatment

Monkey groups[a]	Brain regions	C1q$^+$	Ki67$^+$	C1q$^+$/Ki67$^+$
Ctrl	Insular cortex	2.3 ± 2.2	0.1 ± 0.1	0.1 ± 0.1
	Occipital cortex	4.9 ± 2.6	0	0
	Basofrontal cortex	1.7 ± 1.3	0.1	0.1
	Striatum	1.0 ± 0.2	0.2 ± 0.1	0.1 ± 0.1
	Corpus callosum	1.2 ± 0.2	0.7 ± 0.5	0.4 ± 0.3
SIV,−AIDS	Insular cortex	6.8 ± 3.7	0.9 ± 0.8	0.9 ± 0.7
	Occipital cortex	12.9 ± 3.2[b]	1.4 ± 0.7	1.3 ± 0.8
	Basofrontal cortex	10.0 ± 5.5[b]	1.3 ± 0.6	1.2 ± 0.6
	Striatum	7.9 ± 1.9[b]	1.6 ± 0.8	1.6 ± 0.7
	Corpus callosum	8.8 ± 1.6[b]	6.0 ± 3.1[b]	5.3 ± 2.5[b]
SIV,+AIDS	Insular cortex	40.6 ± 5.6[c]	14.0 ± 7.0[d]	12.7 ± 6.3[c]
	Occipital cortex	48.3 ± 9.4[c]	7.3 ± 4.1[d]	6.9 ± 4.0[c]
	Basofrontal cortex	40.3 ± 6.9[c]	8.6 ± 3.7[d]	8.1 ± 3.4[c]
	Striatum	44.4 ± 7.5[c]	17.8 ± 7.0[d]	16.5 ± 7.0[d]
	Corpus callosum	38.6 ± 11.6[c]	18.4 ± 4.8[c]	17.6 ± 5.6[d]
SIV,+AIDS,+ddG	Insular cortex	6.8 ± 2.8	8.1 ± 5.1[d]	2.4 ± 1.1[b]
	Occipital cortex	9.1 ± 4.3	7.3 ± 3.6[d]	3.5 ± 1.7[b]
	Basofrontal cortex	8.2 ± 3.2[b]	7.3 ± 2.1[d]	3.7 ± 1.2[b]
	Striatum	5.2 ± 2.0[b]	8.8 ± 4.9[d]	2.7 ± 1.3[b]
	Corpus callosum	5.2 ± 2.1[b]	6.8 ± 3.1[b]	2.7 ± 0.7[b]

ANOVA and the post hoc Newman–Keuls Multiple Comparison Test are used to evaluate statistical differences.
[a] Data expressed as mean number (±SEM) of C1q-, Ki67-positive, or C1q-/Ki67-co-positive cells per 0.1 mm^2 area.
[b] Statistically significantly different only as compared to Ctrl group for the same brain area ($P < 0.05$).
[c] Statistically significantly different as compared to the other animal groups for the same brain area ($P < 0.05$).
[d] Statistically significantly different only as compared to Ctrl and SIV,−AIDS groups for the same brain area ($P < 0.05$).

oligodendocytes (Figs. 2C, D). C1q protein was not seen in the cytoplasm of neuronal perikarya and was undetectable in endothelial cells (Figs. 2E, F).

Additionally, co-localization experiments were performed by combining IHC and ISH. C1q A mRNA hybridization signals were found in isolectin-positive microglia, macrophages, and multi-

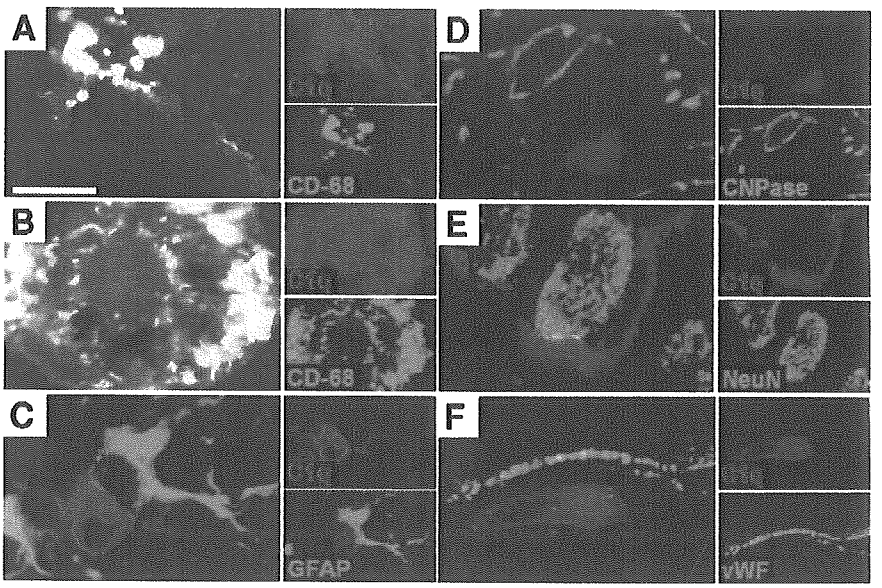

Fig. 2. Identification of C1q-positive cell types. Confocal laser scanning images of double immunofluorescence demonstrating co-existence of C1q (red) with the activation marker CD-68 (green) in a single microglia/macrophage and in a multinucleated giant cell (A and B) and segregation of C1q (red) with the established markers of brain resident cells (green)-glial fibrillary acid protein (GFAP) for astrocytes (C), 2′,3′-cyclic nucleotide-3′-phosphodiesterase (CNPase) for oligodendrocytes (D), neuronal antigen NeuN for neurons (E), and van Willebrand factor (vWF) for endothelial cells (F). A minimum of about 500 cells were examined for each cell type for each SIV-infected animal with AIDS (SIV,+AIDS) to make definitive statements. Scale bar in A for A–F is 10 μm in single-colored micrographs and 5 μm in micrographs with overlayed colors.

nucleated giant cells (Figs. 3A, B) in brains of monkeys with AIDS, but were totally absent from isolectin-positive endothelial cells (Figs. 3A, B). C1q protein was co-localized with its mRNA as shown for subependymal macrophages and macrophages adherent on the ependymal surface (Fig. 3C, D). Double ISH revealed the presence of transcripts encoding all three chains of C1q in diffusely distributed as well as in nodule and syncytium forming microglia/macrophages (Figs. 4A, B) and confirmed the absence of C1q biosynthesis in endothelial cells and neuronal cell bodies (Fig. 4C). Ependymal cells neither exhibited hybridization signals for C1q mRNA nor were they C1q-immunoreactive. In all animal groups, C1q A, B, and C mRNAs were not detected in neurons. However, in the absence of neuronal synthesis of C1q, a variable number of neurons throughout the brain exhibited deposition of immunopositive C1q on the surface membrane of their somata and processes (Figs. 5A, B), both in control and in infected animals, with no obvious difference between the four experimental groups.

Relationship of C1q expression to cell proliferation and influence of antiretroviral treatment

To determine whether the level of C1q expression is due to SIV-induced cell proliferation, double IHC for C1q and the nuclear proliferation marker Ki67 was carried out. Ki67-immunostaining revealed very few proliferating cells which were mainly found in perivascular areas, both in the brains of control and asymptomatically infected animals. The clinical manifestation of disease was characterized by an increase of proliferation in perivascular areas and an appearance of proliferating cells adhering to the luminal endothelium as well as by an induction of diffuse cell proliferation in the brain parenchyma (Fig. 6). To determine the correlation between C1q-positive cells and Ki67-positive proliferating cells, computer-assisted comparative cell counting was performed as demonstrated for the insular, occipital, and basofrontal cortices, for the striatum and for the corpus callosum (Table 3). In monkey brains of the SIV,+AIDS group, 92–97% of proliferating cells were C1q-immunoreactive. In antiretrovirally treated animals, the number of cells labeled for C1q alone or co-labeled for C1q and Ki67 was similar to that in infected animals without AIDS. Antiretroviral treatment had no significant influence on the total number of Ki67-positive cells as compared to untreated AIDS-diseased animals except for the corpus callosum (Figs. 6A–D; Table 3). However, parenchymal accumulation of Ki67-positive proliferating cells seen in untreated animals was absent in all four animals receiving antiretroviral treatment. In contrast, the vessel-associated cell proliferation seen in the SIV,+AIDS group was largely unaffected by the antiretroviral treatment (Table 4). The different proliferating or non-proliferating C1q-positive cell types observed in the brain of monkeys with AIDS were assessed by double IHC for C1q and Ki67 (Fig. 7).

Adherence of C1q-positive cells on the endothelium in late stage of SIV infection and influence of antiretroviral treatment

Adherence of inflammatory cells on the luminal endothelium is regarded as a morphological sign for infiltration of cells through the blood–brain barrier (Williams and Hickey, 1995). Our quantitative analysis revealed an increase in the number of C1q-immunostained cells adhering on the luminal side of the endothelium in the brain of monkeys with AIDS ($P < 0.05$), especially in areas with accumulation of macrophages and multinucleated giant cells known as hallmarks of productive SIV infection. Apparently, these cells were truly adherent and in the progress of infiltrating into the brain as they were not washed away by the transcardial perfusion prior to or during fixation procedures. Antiretroviral treatment was found to reduce the number of C1q-positive cells attached to the endothelium (Table 5).

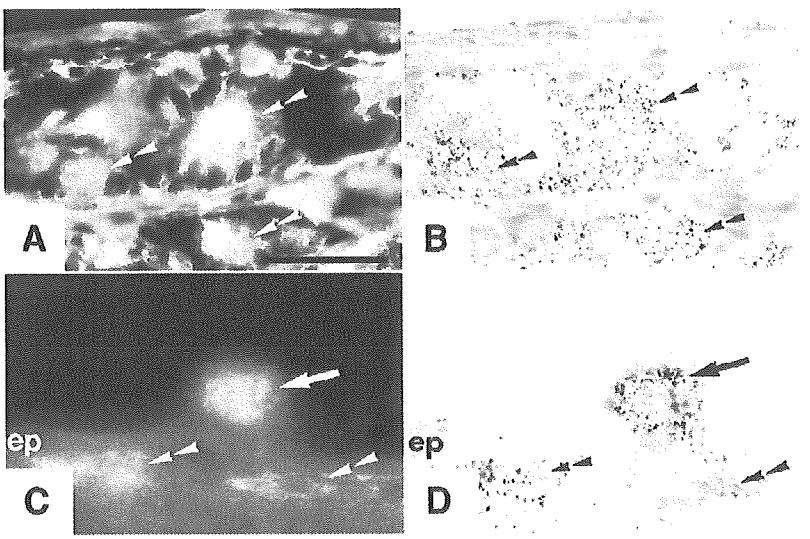

Fig. 3. Combinatorial in situ hybridization and immunofluorescence on identical brain sections of an untreated monkey with AIDS. (A and B) Hybridization signals for C1q A mRNA are present in isolectin-positive macrophages and multinucleated giant cells (double arrowheads) but not in isolectin-positive endothelial cells. (C and D) In situ hybridization signals for C1q A mRNA in C1q-immunopositive cells adherent on the ependymal surface (arrows) and lying subependymally (double arrowheads). Note the absence of C1q expression from ependymal cells (ep), which are negative for both C1q protein and C1q mRNA. Scale bar in A for A–D is 10 μm.

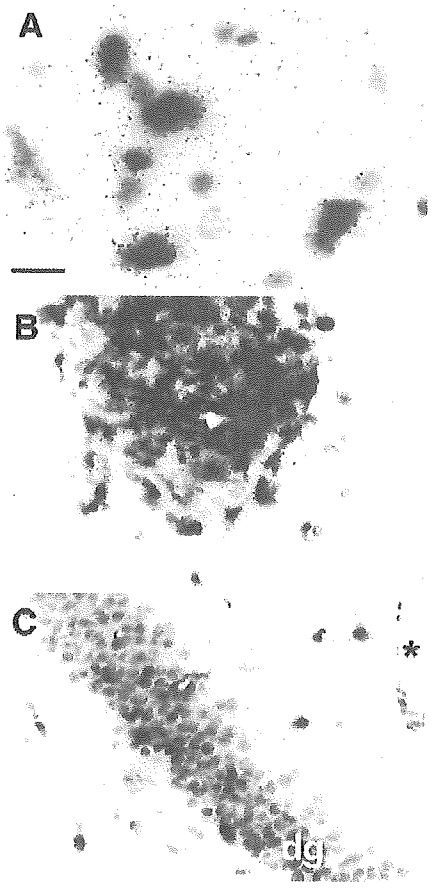

Fig. 4. Co-hybridization for mRNA encoding C1q peptide chains A, B, and C in the brain of monkeys with AIDS. (A) Transcript for C1q chains B (dark blue reaction) and C (silver grains) in diffusely distributed microglia/macrophages. (B and C) Message for C1q chains A (blue reaction) and C (silver grains) is present in nodule and giant cell forming as well as in diffusely distributed macrophages. Note the absence of transcripts of C1q A and C1q C chains from dentate gyrus (dg) neurons and endothelia of a blood vessel (asterisk). Scale bar in A for A–C is 50 μm.

Brain viral burden and CNS-selective antiretroviral treatment

The effect of antiretroviral treatment on brain viral burden is summarized in Table 1. There was little evidence that the SIV replicated in the CNS in the asymptomatic stage of infection. SIV RNA- and SIV glycoprotein *gp41*-positive cells were mainly detected in the animals with clinical symptoms of AIDS and with SIV encephalitis. Only cells of the microglia/macrophage-lineage were found to contain SIV RNA and *gp41* protein. There was no evidence for the presence of SIV RNA or SIV gp41 immunoreactivity in astrocytes or endothelial cells under our different experimental conditions. Co-staining experiments for *gp41* and C1q revealed that nearly all C1q-positive multinucleated giant cells were also stained for virus *gp41* (>95%). Most C1q-positive macrophages were *gp41*-positive (70–80%). The microglia compartment had the lowest number of cells double labeled for C1q and *gp41* (<10%; Fig. 8). Antiviral treatment markedly reduced the number of SIV RNA- and *gp41*-positive cells. The effects of antiviral treatment on viral burden and RCA-120- or CD-68-stained mononuclear reactions in the brain are summarized in Table 1.

Discussion

This study describes the plasticity of C1q expression in the brain of rhesus monkeys during the course of simian immunodeficiency virus infection. A striking feature is that C1q was globally upregulated in early asymptomatic stage of SIV disease. This early phase of C1q increase was followed by an enhanced C1q expression when clinical symptoms manifested. The former was an increase in the number of C1q-immunoreactive brain resident cells, the latter was a result of C1q gene transcription as well as of proliferation and infiltration of C1q-positive cells in the brain. The susceptibility to antiretroviral treatment with the lipophilic 6-chloro-2′,3′-dideoxyguanosine demonstrated that brain C1q synthesis was directly related to brain SIV burden.

In our study, using IHC and ISH and combination of both techniques, we identified exclusively cells of the mononuclear lineage–microglia, macrophages, and multinucleated giant cells–as the sources of cerebral C1q biosynthesis. Similar observations have been previously reported in the Borna-infected rat brain (Dietzschold et al., 1995). By demonstrating that C1q protein and the three mRNAs encoding the three C1q chains were co-regulated, we provide evidence that functionally intact C1q is synthesized in the brain during SIV infection. Before manifestation of clinical AIDS, virus burden and signs of productive inflammation in the brain were low, and C1q was predominantly found in microglia. In contrast, the late stage was characterized by high viral burden and encephalitis in the brain, and C1q was also found in resident and infiltrating macrophages as well as in multinucleated giant cells.

Antiretroviral treatment of AIDS-diseased monkeys reduced cerebral virus burden and virus-induced encephalitis which resulted in substantial decline of C1q expression in the brain as compared to AIDS-diseased animals receiving no antiretroviral treatment. As the animal receiving 6-Cl-ddG alone (MO89) was effectively treated with respect to reduction of brain virus burden and the degree of SIV-induced encephalitis, we conclude that 6-Cl-ddG is effective independent of pretreatment with ddI.

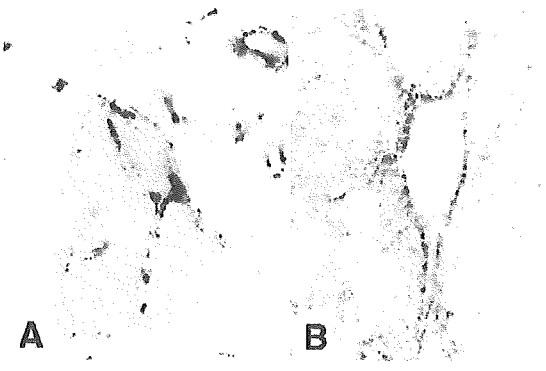

Fig. 5. High-power micrographs demonstrating neuronal surface staining of C1q as shown for a neuron of the substantia nigra pars compacta (A) and a motoneuron of the thoracic spinal cord (B) of a control monkey. Note that the cytoplasm of the perikarya and processes is free from C1q. All monkey brains of all experimental groups demonstrated same staining pattern without obvious difference.

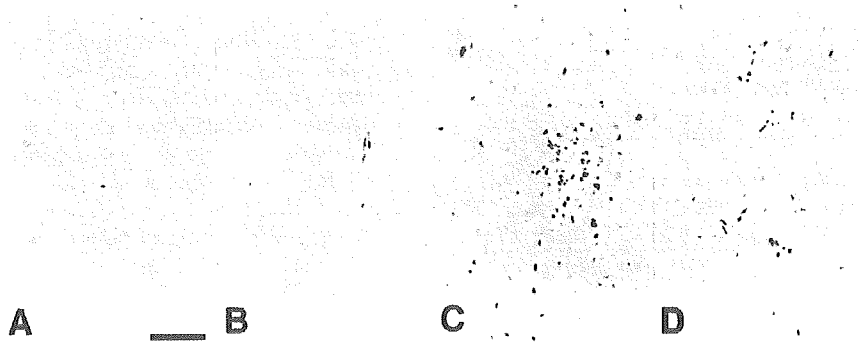

Fig. 6. Effect of antiviral treatment with 6-Cl-ddG on nuclear proliferation antigen Ki67 in the monkey insular cortex. Note the low number of Ki67-stained cell nuclei in the Ctrl and SIV,−AIDS groups (A and B) but high levels in the AIDS-diseased animal groups (C and D). Untreated symptomatic monkeys demonstrate a more diffuse and nodular Ki67 staining (C) in contrast to antiretrovirally treated monkeys exhibiting AIDS which exhibit mainly a vasculature-associated staining for Ki67 (D). Scale bar in A for A–D is 100 μm.

Apparently, the degree of increase in C1q expression correlates with the viral load in the brain. The key observation to be derived from the CNS-permeant and systemic antiretroviral therapy is the tight linkage between brain virus burden and C1q expression in the microglial/macrophage cellular compartment, both positively in late-stage (untreated) AIDS, and negatively in late-stage AIDS accompanied by CNS-permeant plus systemic antiretroviral therapy. Noteworthy, the C1q increase in microglia during clinical latency suggests that microglial activation and neuroinflammatory damage in the brain occur early during SIV infection perhaps through the early presence of SIV in the CNS, although SIV is not replicating in this stage. The effect of 6-Cl-ddG appeared to be cell-specific. It was shown to reduce SIV-induced upregulation of C1q expression in microglial cells and to completely abolish the appearance of C1q expressing macrophages and multinucleated giant cells. Thus, signs of productive inflammation (Budka, 1986; Dickson, 1986; Kato et al., 1987; Lane et al., 1996; Lifson et al., 1986; Williams et al., 2001) and the appearance of SIV RNA- and SIV protein-positive cells were markedly decreased by 6-Cl-ddG. Antiretroviral treatment significantly reduced but did not abolish microglial activation. Interestingly, the antiretroviral treatment selectively reduced SIV-induced proliferation of brain parenchymal cells and down-regulated C1q expression in microglia and parenchymal macrophages. In contrast, juxtavascular proliferation was partly resistant to antiretroviral treatment while an increase of C1q biosynthesis in intravascular and perivascular cells of the monocyte/macrophage-lineage was blocked by the treatment. The dissociated effectiveness of 6-Cl-ddG treatment in CNS tissues and the relative resistance to that treatment in peripheral cells may be explained by the better uptake of the lipophilic 6-Cl-ddG by CNS cells.

The increased local synthesis of C1q in brain resident and invading cells is likely to be important in the complement-mediated opsonization of SIV (Speth et al., 2002) and modulation of phagocytosis by endothelial cells, macrophages, monocytes, and microglia (Bobak et al., 1987). In addition to pro-

Table 4
Effect of antiretroviral treatment on parenchymal and vasculature-associated cell proliferation

Monkey groups[a]	Brain region	Parenchymal	Vasculature associated[b]
SIV,+AIDS	Insular cortex	8.8 ± 2.1	5.2 ± 1.1
	Occipital cortex	4.6 ± 1.5	2.4 ± 0.7
	Striatum	10.3 ± 1.5	7.6 ± 3.0
SIV,+AIDS,+ddG	Insular cortex	2.4 ± 0.5[c]	5.6 ± 1.9
	Occipital cortex	2.0 ± 0.3[c]	5.2 ± 1.4
	Striatum	1.9 ± 0.5[c]	6.9 ± 1.9

Unpaired, two-tailed Student's t test is used to evaluate statistical differences.

[a] Data expressed as mean number (±SEM) of Ki67-positive cell nuclei per 0.1 mm^2 area.

[b] Proliferating cells demonstrating perivascular or intraluminal endothelial adherent staining.

[c] Statistically significantly reduced as compared to the untreated group for the same brain area ($P < 0.05$).

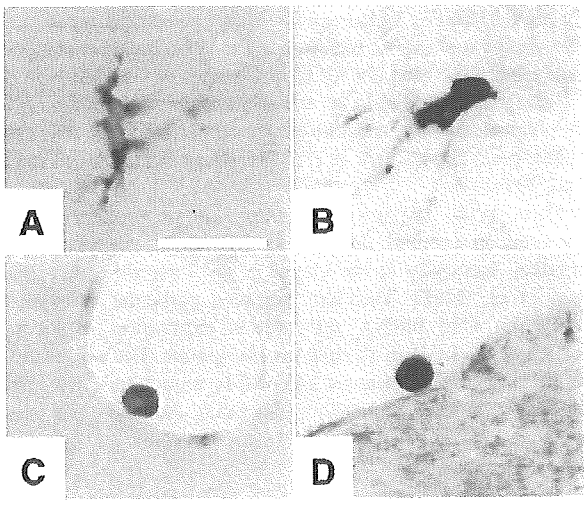

Fig. 7. C1q-positive cells with respect to proliferating and non-proliferating activity in the brain of monkeys with AIDS revealed by double immunohistochemistry for C1q and Ki67. Parenchymal microglia/macrophages (brown, A and B) and vessel-attached monocytes (brown, C and D) demonstrating no Ki67 staining (A and C) or clear nuclear Ki67 staining (nuclear dark blue, B and D). Note that the cell in (B) demonstrates nuclear Ki67 staining typical for a cell undergoing mitosis. Scale bar in A for A–D is 10 μm.

Table 5
Quantitative analysis of C1q-immunopositive cells adhering on the intraluminal surface of cerebrovascular endothelium

Monkey groups[a]	Insular cortex	Occipital cortex	Striatum
Ctrl	0	0	0
SIV,−AIDS	0.3 ± 0.2	0.3 ± 0.2	0.2 ± 0.2
SIV,+AIDS	3.9 ± 1.4[b]	4.6 ± 1.4[b]	4.8 ± 1.6[b]
SIV,+AIDS,+ddG	1.0 ± 0.6	1.2 ± 0.7	0.6 ± 0.3

ANOVA and the post hoc Newman–Keuls Multiple Comparison Test are used to evaluate statistical differences.

[a] Data expressed as mean number (±SEM) of C1q-positive cells per 0.1 mm^2 area.

[b] Statistically significantly different as compared to the other animal groups for the same brain area ($P < 0.05$).

inflammatory effect of C1q on its own, the activation of complement components downstream of C1q may generate soluble mediators which could trigger infiltration of inflammatory cells into the brain directly by chemoattractant properties of complement anaphylatoxins and cleavage products to complement receptor bearing cells (Ghebrehiwet et al., 1995; Kuna et al., 1996; Leigh et al., 1998; Speth et al., 1997) and/or indirectly by upregulation of adhesion molecules like the endothelial P-selectin or chemokines like MCP-1 (Mulligan et al., 1997; van den Berg et al., 1998).

Therefore, we propose that C1q levels in brain are a useful indicator for the severity of inflammatory reactions during lentiviral infections as well as for virus burden. This is of potential significance for monitoring progression and amelioration of SIV-associated neurological disease and for the prognosis of therapeutic interventions by determining C1q levels in the CSF. Changes in CSF levels of mediators of the immune response following antiretroviral therapy in AIDS had been reported previously for immediate early proteins like neopterin and β_2-microglobulin, neurotoxins like quinolinic acid, cytokines and cytokine receptors like MCP-1, TNF-α ligand and its soluble receptor (Conant et al., 1998; Fuchs et al., 1990; Gulevich et al., 1993; Heyes et al., 1989; Look et al., 2000) but not for C1q. Changes of C1q levels in the CSF had been reported in several degenerative and inflammatory neurological diseases and disease models (Antoine et al., 1986; Schäfer et al., 2000; Smyth et al., 1994; Wajgt et al., 1989; Yamada et al., 1994).

There is an ongoing controversy as to whether C1q is expressed in cerebral neurons in the course of neurological disorders, especially in the human brain (Fonseca et al., 2004; Head et al., 2001). Therefore, we paid particular attention to monitoring C1q mRNA and protein expression in neurons throughout the brain in all experimental groups. The total absence of C1q mRNA from neurons and of C1q immunoreactivity from neuronal cytoplasm throughout the brain found in this study provides no evidence that neurons synthesize C1q in normal and diseased rhesus monkey brain. This is in accordance with our previous studies on rodents also showing restriction of C1q expression to microglial/macrophage cells both after CNS virus inflammation and after cerebral ischemia or toxic lesion of the blood–brain barrier (Dietzschold et al., 1995; Lynch et al., 2004; Schäfer et al., 2000).

The deposition of C1q on the outer surfaces seen in the present study in some neurons throughout brains of all experimental groups may be due to deposition of extrinsic C1q most likely coming from local production or from serum through local leakages of the blood–brain barrier. This deposition of C1q on neuronal surfaces may be taken as evidence that a putative C1q receptor is expressed on some neurons (Eggleton et al., 2000; Kishore and Reid, 2000). Our results are in some concordance with immunohistochemical data by Speth et al. (2004) also showing C1q-immunopositive microglial/macrophage cells, but unlike these authors, our study clearly excludes astrocytes and neurons as a source of C1q biosynthesis and provides no evidence that deposition of C1q on neuronal surfaces is causally related to SIV infection.

C1q is one of several response genes of the monocyte/macrophage arm of innate immunity which is regulated during HIV/SIV infection as recently evaluated using DNA array technology in the accelerated CD8-depletion model of SIV-infected rhesus macaques (Roberts et al., 2003). Among them, indoleamine 2,3-dioxygenase is upregulated like C1q in SIV brain disease and is sensitive to antiretroviral treatment (Depboylu et al., 2004). We obtained no evidence for the presence of SIV RNA and protein in astrocytes that certainly exhibit activation during SIV infection as shown previously (Weihe et al., 1993). Astrocytes are likely involved in the retroviral neuropathogenesis, but most evidence does not support widespread infection of them in vivo. For humans, it had been primarily pediatric cases with massive HIV brain infection that had shown infection of astrocytes (Saito et al., 1994; Tornatore et al., 1994). Otherwise, such findings had been observed mainly in vitro/ex vivo, or in models such as the pig-tailed macaque accelerated model characterized by massive CNS infection and very short term disease (Overholser et al., 2003).

In summary, our study provides clear evidence that C1q synthesis is induced in brain resident and infiltrating immune cells following SIV infection and correlates with brain virus load as well as clinical manifestation of simian AIDS. The relationship between C1q expression in microglia/macrophages and multinucleated giant cells, and virus burden may ultimately be useful in revealing the functional association of inflammatory and virological markers during lentiviral infection of the brain, and therefore the role of each in motor/cognitive dysfunction associated with lentiviral infection.

Fig. 8. Double immunofluorescence confocal images demonstrating co-existence of C1q (red) with the SIV glycoprotein *gp41* (green) in a microglia in the brain of an untreated AIDS-diseased animal (A–C). Scale bar in A for A–C is 10 μm.

Acknowledgments

This study was supported by a grant of the Volkswagen Foundation to L. E. Eiden and E. Weihe and the German Research Foundation (Schwerpunkt Mikroglia) to E. Weihe and W. J. Schwaeble. For excellent technical work, we thank R. Vertesi and D. Huddleston from L. E. Eiden's lab as well as E. Rodenberg-Frank, M. Zibuschka, T. Henke, and H. Hlawaty from E. Weihe's lab. For expert photographic assistance, we are indebted to H. Schneider from E. Weihe's lab. Parts of this study were presented at the 31st Annual Meeting of the Society for Neuroscience in San Diego, USA (Depboylu et al., 2001).

References

Antoine, J.C., Michel, D., Lamelin, J.P., Laurent, B., Schott, B., 1986. Cerebrospinal fluid and serum immune complex in acute inflammatory polyneuritis. Detection by C1q binding assay. Acta Neurol. Scand. 73, 477–480.

Bissel, S.J., Wang, G., Ghosh, M., Reinhart, T.A., Capuano III, S., Stefano Cole, K., Murphey-Corb, M., Piatak Jr., M., Lifson, J.D., Wiley, C.A., 2002. Macrophages relate presynaptic and postsynaptic damage in simian immunodeficiency virus encephalitis. Am. J. Pathol. 160, 927–941.

Bobak, D.A., Gaither, T.A., Frank, M.M., Tenner, A.J., 1987. Modulation of FcR function by complement: subcomponent C1q enhances the phagocytosis of IgG-opsonized targets by human monocytes and culture-derived macrophages. J. Immunol. 138, 1150–1156.

Budka, H., 1986. Multinucleated giant cells in the brain: a hallmark of the acquired immunodeficiency syndrome (AIDS). Acta Neuropathol. (Berl.) 69, 253–256.

Conant, K., Garzino-Demo, A., Nath, A., McArthur, J.C., Halliday, W., Power, C., Gallo, R.C., 1998. Major induction of monocyte chemoattractant protein-1 in HIV-1 Tat-stimulated astrocytes and elevation in AIDS dementia. Proc. Natl. Acad. Sci. U. S. A. 95, 3117–3121.

da Cunha, A., Rausch, D.M., Eiden, L.E., 1995. An early increase in somatostatin mRNA expression in the frontal cortex of rhesus monkeys infected with simian immunodeficiency virus. Proc. Natl. Acad. Sci. U. S. A. 92, 1371–1375.

Depboylu, C., Reinhart, T.A., Schwaeble, W.J., Mitsuya, H., Eiden, L.E., Weihe, E., 2001. Brain C1q is increased in SIV infection in the rhesus macaque, and is directly related to brain virus burden. Soc. Neurosci. Abstr. 27:1745, 657.16.

Depboylu, C., Reinhart, T.A., Takikawa, O., Imai, Y., Maeda, H., Mitsuya, H., Rausch, D., Eiden, L.E., Weihe, E., 2004. Brain virus burden and indoleamine-2,3-dioxygenase during lentiviral infection of rhesus monkey are concomitantly lowered by 6-chloro-2′,3′-dideoxyguanosine. Eur. J. Neurosci. 19, 2997–3005.

Dickson, D.W., 1986. Multinucleated giant cells in acquired immunodeficiency syndrome encephalopathy. Arch. Pathol. Lab. Med. 110, 967–968.

Dietzschold, B., Schwaeble, W., Schäfer, M.K.-H., Petry, F., Zheng, Y., Fink, T., Loos, M., Weihe, E., 1995. The expression of C1q, a subcomponent of the rat complement system is dramatically enhanced in brains of rats with either Borna disease or experimental allergic encephalomyelitis. J. Neurol. Sci. 130, 11–16.

Ebenbichler, C.F., Thielens, N.M., Vornhagen, R., Marschan, P., Arlaud, G.J., Dierich, M.P., 1991. Human immunodeficiency virus type 1 activates the classical pathway of complement by direct C1 binding through specific sites in the transmembrane glycoprotein gp 41. J. Exp. Med. 174, 1417–1424.

Eggleton, P., Tenner, A.J., Reid, K.B., 2000. C1q receptors. Clin. Exp. Immunol. 120, 406–412.

Farkas, I., Takahashi, M., Fukuda, A., Yamamoto, N., Akatsu, H., Baranyi, L., Tateyama, H., Yamamoto, T., Okada, N., Okada, H., 2003. Complement C5a receptor-mediated signaling may be involved in neurodegeneration in Alzheimer's disease. J. Immunol. 170, 5764–5771.

Fonseca, M.I., Kawas, C.H., Troncoso, J.C., Tenner, A.J., 2004. Neuronal localization of C1q in preclinical Alzheimer's disease. Neurobiol. Dis. 15, 40–46.

Fuchs, D., Moller, A.A., Reibnegger, G., Stockle, E., Werner, E.R., Wachter, H., 1990. Decreased serum tryptophan in patients with HIV-1 infection correlates with increased serum neopterin and with neurologic/psychiatric symptoms. Acquir. Immune Defic. Syndr. 3, 873–876.

Fujii, Y., Mukai, R., Mori, K., Akari, H., Otani, I., Ono, F., Kojima, E., Takasaka, M., Machida, M., Murakami, K., Yoshikawa, Y., 1997a. Efficacy of 6-chloro-2′,3′-dideoxyguanosine (6-Cl-ddG) on rhesus macaque monkeys chronically infected with simian immunodeficiency virus (SIVmac239). J. Acquir. Immune Defic. Syndr. Hum. Retrovirol. 16, 313–317.

Fujii, Y., Mukai, R., Murayama, Y., Akari, H., Machida, M., Mori, K., Takasaka, M., Murakami, K., Yoshikawa, Y., 1997b. Efficacy of 6-chloro-2′,3′-dideoxyguanosine (6-Cl-ddG) on an ARC/AIDS rhesus macaque (*Macaca mulatta*) infected with simian immunodeficiency virus. Exp. Anim. 46, 83–87.

Fujii, Y., Mukai, R., Akari, H., Machida, M., Mori, K., Takasaka, M., Kojima, E., Murakami, K., Yoshikawa, Y., 1998. Antiviral effects of 6-chloro-2′,3′-dideoxyguanosine in rhesus monkeys acutely infected with simian immunodeficiency virus. Antivir. Chem. Chemother. 9, 85–92.

Ghebrehiwet, B., Kew, R.R., Gruber, B.L., Marchese, M.J., Peerschke, E.I., Reid, K.B., 1995. Murine mast cells express two types of C1q receptors that are involved in the induction of chemotaxis and chemokinesis. J. Immunol. 155, 2614–2619.

Glass, J.D., Fedor, H., Wesselingh, S.L., McArthur, J.C., 1995. Immunocytochemical quantitation of human immunodeficiency virus in the brain: correlations with dementia. Ann. Neurol. 38, 755–762.

Gulevich, S.J., McCutchan, J.A., Thal, L.J., Kirson, D., Durand, D., Wallace, M., Mehta, P., Heyes, M.P., Grant, I., 1993. Effect of antiretroviral therapy on the cerebrospinal fluid of patients seropositive for the human immunodeficiency virus. J. Acquir. Immune Defic. Syndr. 6, 1002–1007.

Hawkins, M.E., Mitsuya, H., McCully, C.L., Godwin, K., Murakami, K., Poplack, D.G., Balis, F.M., 1995. Plasma and cerebrospinal fluid pharmacokinetics of dideoxypurine nucleoside analogs in rhesus monkeys. Antimicrob. Agents Chemother. 39, 1259–1264.

Head, E., Azizeh, B.Y., Lott, I.T., Tenner, A.J., Cotman, C.W., Cribbs, D.H., 2001. Complement association with neurons and beta-amyloid deposition in the brains of aged individuals with down syndrome. Neurobiol. Dis. 8, 252–265.

Heyes, M.P., Rubinow, D., Lane, C., Markey, S.P., 1989. Cerebrospinal fluid quinolinic acid concentrations are increased in acquired immune deficiency syndrome. Ann. Neurol. 26, 275–277.

Kato, T., Hirano, A., Llena, J.F., Dembitzer, H.M., 1987. Neuropathology of the acquired immune deficiency syndrome (AIDS) in 53 autopsy cases with particular emphasis on microglial nodules and multinucleated giant cells. Acta Neuropathol. 73, 287–294.

Kent, K.A., Rud, E., Cororan, T., Powell, C., Thiriart, C., Collignon, C., Stott, E.J., 1992. Identification of two neutralizing and eight non-neutralizing epitopes on simian immunodeficiency virus envelope using monoclonal antibodies. AIDS Res. Hum. Retroviruses 8, 1147–1151.

Kishore, U., Reid, K.B., 2000. C1q: structure, function and receptors. Immunopharmacology 49, 159–170.

Klein, M.A., Kaeser, P.S., Schwarz, P., Weyd, H., Xenarios, I., Zinkernagel, R.M., Carroll, M.C., Verbeek, J.S., Botto, M., Walport, M.J., Molina, H., Kalinke, U., Acha-Orbea, H., Aguzzi, A., 2001. Complement facilitates early prion pathogenesis. Nat. Med. 7, 488–492.

Kovacs, G.G., Gasque, P., Strobel, T., Lindeck-Pozza, E., Strohschneider, M., Ironside, J.W., Budka, H., Guentchev, M., 2004. Complement activation in human prion disease. Neurobiol. Dis. 15, 21–28.

Kuna, P., Iyer, M., Peerschke, E.I., Kaplan, A.P., Reid, K.B., Ghebrehiwet,

B., 1996. Human C1q induces eosinophil migration. Clin. Immunol. Immunopathol. 81, 48–54.
Lane, J.H., Sasseville, V.G., Smith, M.O., Vogel, P., Pauley, D.R., Heyes, M.P., Lackner, A.A., 1996. Neuroinvasion by simian immunodeficiency virus coincides with increased numbers of perivascular macrophages/microglia and intrathecal immune activation. J. Neurovirol. 2, 423–432.
Leigh, L.E., Ghebrehiwet, B., Perera, T.P., Bird, I.N., Strong, P., Kishore, U., Reid, K.B., Eggleton, P., 1998. C1q-mediated chemotaxis by human neutrophils: involvement of gC1qR and G-protein signalling mechanisms. Biochem. J. 330, 247–254.
Li, Q., Eiden, L.E., Cavert, W., Reinhart, T.A., Rausch, D.M., Murray, E.A., Weihe, E., Haase, A.T., 1999. Increased expression of nitric oxide synthase and dendritic injury in simian immunodeficiency virus encephalitis. J. Hum. Virol. 2, 139–145.
Lifson, J.D., Reyes, G.R., McGrath, M.S., Stein, B.S., Engelmann, E.G., 1986. AIDS retrovirus induced cytopathology: giant cell formation and involvement of CD4 antigen. Science 232, 1123–1127.
Lipton, S.A., Sucher, N.J., Kaiser, P.K., Dreyer, E.B., 1991. Synergistic effects of HIV coat protein and NMDA receptor-mediated neurotoxicity. Neuron 7, 111–118.
Look, M.P., Altfeld, M., Kreuzer, K.A., Riezler, R., Stabler, S.P., Allen, R.H., Sauerbruch, T., Rockstroh, J.K., 2000. Parallel decrease in neurotoxin quinolinic acid and soluble tumor necrosis factor receptor p75 in serum during highly active antiretroviral therapy of HIV type 1 disease. AIDS Res. Hum. Retroviruses 16, 1215–1221.
Luabeya, M.-K., Dallasta, L.M., Achim, C.L., Pauza, C.D., Hamilton, R.L., 2000. Blood–brain barrier disruption in simian immunodeficiency virus encephalitis. Neuropathol. Appl. Neurobiol. 26, 454–462.
Luthert, P.J., Montgomery, M.M., Dean, A.F., Cook, R.W., Baskerville, A., Lantos, P.L., 1995. Hippocampal neuronal atrophy occurs in rhesus macaques following infection with simian immunodeficiency virus. Neuropathol. Appl. Neurobiol. 21, 529–534.
Lynch, N.J., Willis, C.L., Nolan, C.C., Roscher, S., Fowler, M.J., Weihe, E., Ray, D.E., Schwaeble, W.J., 2004. Microglial activation and increased synthesis of complement component C1q precedes blood–brain barrier dysfunction in rats. Mol. Immunol. 40, 709–716.
Montefiori, D.C., Robinson, W.E., Hirsch, V.M., Modliszewski, A., Mitchell, W.M., Johnson, P.R., 1990. Antibody-dependent enhancement of simian immnodeficiency virus (SIV) infection in vitro by plasma from SIV-infected rhesus macaques. J. Virol. 64, 113–119.
Mulligan, M.S., Schmid, E., Till, G.O., Hugli, T.E., Friedl, H.P., Roth, R.A., Ward, P.A., 1997. C5a-dependent up-regulation in vivo of lung vascular P-selectin. J. Immunol. 158, 1857–1861.
Murray, E.A., Rausch, D.M., Lendvay, J., Sharer, L.R., Eiden, L.E., 1992. Cognitive and motor impairments associated with SIV infection in rhesus monkeys. Science 255, 1246–1249.
Overholser, E.D., Coleman, G.D., Bennett, J.L., Casaday, R.J., Zink, M.C., Barber, S.A., Clements, J.E., 2003. Expression of simian immunodeficiency virus (SIV) nef in astrocytes during acute and terminal infection and requirement of nef for optimal replication of neurovirulent SIV in vitro. J. Virol. 77, 6855–6866.
Perricone, R., Fontana, L., De Carolis, C., Carini, C., Sirianni, M.C., Aiuti, F., 1987. Evidence for activation of complement in patients with AIDS-related complex (ARC) and/or lymphadenopathy syndrome (LAS). Clin. Exp. Immunol. 70, 500–507.
Power, C., Gill, M.J., Johnson, R.T., 2002. Progress in clinical neurosciences: the neuropathogenesis of HIV infection: host–virus interaction and the impact of therapy. Can. J. Neurol. Sci. 29, 19–32.
Reinhart, T.A., Rogan, M.J., Huddleston, D., Rausch, D.M., Eiden, L.E., Haase, A.T., 1997. Simian immunodeficiency virus burden in tissues and cellular compartments during clinical latency and AIDS. J. Infect. Dis. 176, 1198–1208.
Roberts, E.S., Zandonatti, M.A., Watry, D.D., Madden, L.J., Henriksen, S.J., Taffe, M.A., Fox, H.S., 2003. Induction of pathogenic sets of genes in macrophages and neurons in NeuroAIDS. Am. J. Pathol. 162, 2041–2057.
Robinson Jr., W.E., Montefiori, D.C., Mitchell, W.M., 1988. Antibody-dependent enhancement of human immunodeficiency virus type 1 infection. Lancet 1, 790–794.
Robinson Jr., W.E., Montefiori, D.C., Mitchell, W.M., Prince, A.M., Alter, H.J., Dreesmann, G.R., Eichberg, J.W., 1989. Antibody-dependent enhancement of human immunodeficiency virus type 1 (HIV-1) infection in vitro by serum from HIV-1-infected and passively immunized chimpanzees. Proc. Natl. Acad. Sci. U. S. A. 86, 4710–4714.
Robinson, W.E., Montefiori, D.C., Mitchell, W.M., 1990. Complement-mediated antibody-dependent enhancement of HIV-1 infection requires CD4 and complement receptors. Virology 175, 600–604.
Rohrenbeck, A.M., Bette, M., Hooper, D.C., Nyberg, F., Eiden, L.E., Dietzschold, B., Weihe, E., 1999. Upregulation of COX-2 and CGRP expression in resident cells of the Borna disease virus-infected brain is dependent upon inflammation. Neurobiol. Dis. 6, 15–34.
Rostagno, A., Revesz, T., Lashley, T., Tomidokoro, Y., Magnotti, L., Braendgaard, H., Plant, G., Bojsen-Moller, M., Holton, J., Frangione, B., Ghiso, J., 2002. Complement activation in chromosome 13 dementias. Similarities with Alzheimer's disease. J. Biol. Chem. 277, 49782–49790.
Saito, Y., Sharer, L.R., Epstein, L.G., Michaels, J., Mintz, M., Louder, M., Golding, K., Cvetkovich, T.A., Blumberg, B.M., 1994. Overexpression of nef as a marker for restricted HIV-1 infection of astrocytes in postmortem pediatric central nervous tissues. Neurology 44, 474–481.
Schäfer, M.K.-H., Day, R., 1994. In situ hybridization techniques to study processing enzyme expression at the cellular level. Methods Neurosci. 23, 16–44.
Schäfer, M.K.-H., Herman, J.P., Watson, S.J., 1992. In situ hybridization immunohistochemistry. In: London, D. (Ed.), Imaging Drug Action in the Brain. CRC Press, Boca Raton, p. 337.
Schäfer, M.K.-H., Schwaeble, W., Post, C., Salvati, P., Calabresi, M., Sim, R.B., Petry, F., Loos, M., Weihe, E., 2000. Complement C1q is dramatically up-regulated in brain microglia in response to transient global cerebral ischemia. J. Immunol. 164, 5446–5452.
Sellar, G.C., Blake, D.J., Reid, K.B., 1991. Characterization and organization of the genes encoding the A-, B- and C-chains of human complement subcomponent C1q. The complete derived amino acid sequence of human C1q. Biochem. J. 274, 481–490.
Senaldi, G., Peakman, M., McManus, T., Davies, E.T., Tee, D.E., Vergani, D., 1990. Activation of the complement system in human immundeficiency virus infection: relevance of the classical pathway to pathogenesis and disease severity. J. Infect. Dis. 162, 1227–1232.
Shirasaka, T., Murakami, K., Ford, H., Kelley, J., Yoshioka, H., Kojima, E., Aoki, S., Driscoll, J.S., Broder, S., Mitsuya, H., 1990. Halogeneted congeners of 2′,3′-dideoxypurine nucleosides active against HIV in vitro: a new class of lipophilic prodrugs. Proc. Natl. Acad. Sci. U. S. A. 87, 9426–9430.
Singhrao, S., Neal, J., Gasque, P., Morgan, B., Newman, G., 1996. Role of complement in the aetiology of Pick's disease? J. Neuropathol. Exp. Neurol. 55, 578–593.
Smyth, M.D., Cribbs, D.H., Tenner, A.J., Shankle, W.R., Dick, M., Kesslak, J.P., Cotman, C.W., 1994. Decreased levels of C1q in cerebrospinal fluid of living Alzheimer patients correlate with disease state. Neurobiol. Aging 15, 609–614.
Sölder, B.M., Schulz, T.F., Hengster, P., Löwer, J., Larcher, C., Bitterlich, G., Kurth, R., Wachter, H., Dierich, M.P., 1989. HIV and HIV-infected cells differentially activate the human complement system independent of antibody. Immunol. Lett. 22, 135–145.
Speth, C., Kacani, L., Dierich, M.P., 1997. Complement receptors in HIV infection. Immunol. Rev. 159, 49–67.
Speth, C., Dierich, M.P., Gasque, P., 2002. Neuroinvasion by pathogens: a key role of the complement system. Mol. Immunol. 38, 669–679.
Speth, C., Williams, K., Hagleitner, M., Westmoreland, S., Rambach, G., Mohsenipour, I., Schmitz, J., Würzner, R., Lass-Flörl, C., Stoiber, H., Dierich, M.P., Maier, H., 2004. Complement synthesis and activation in the brain of SIV-infected monkeys. J. Neuroimmunol. 151, 45–54.
Tornatore, C., Chandra, R., Berger, J.R., Major, E.O., 1994. HIV-1 infection

of subcortical astrocytes in the pediatric central nervous system. Neurology 44, 481–487.

Tremblay, M., Meloche, S., Sekaly, R.P., Wainberg, M.A., 1990. Complement receptor 2 mediated enhancement of human immunodeficiency virus type 1 infection in Epstein–Barr virus carrying B cells. J. Exp. Med. 171, 1791–1796.

van den Berg, R.H., Faber-Krol, M.C., Sim, R.B., Daha, M.R., 1998. The first subcomponent of complement, C1q, triggers the production of IL-8, IL-6, and monocyte chemoattractant peptide-1 by human umbilical vein endothelial cells. J. Immunol. 161, 6924–6930.

Velazquez, P., Cribbs, D., Poulos, T., Tenner, A., 1997. Aspartate residue 7 in amyloid β-protein is critical for classical complement pathway activation: implications for Alzheimer's disease pathogenesis. Nat. Med. 3, 77–91.

Wajgt, A., Gorny, M., Szczechowski, L., Grzybowski, G., Ochudlo, S., 1989. Effect of immunosuppressive therapy on humoral immune response in multiple sclerosis. Acta Med. Pol. 30, 121–128.

Walsh, M.J., Murray, J.M., 1998. Dual implication of 2′,3′-cyclic nucleotide 3′-posphodiesterase as major autoantigen and C3-complement-binding protein in the pathogenesis of multiple sclerosis. J. Clin. Invest. 101, 1923–1931.

Weihe, E., Nohr, D., Sharer, L., Murray, E., Rausch, D.M., Eiden, L.E., 1993. Cortical astrocytosis in juvenile rhesus monkeys infected with simian immunodeficiency virus. NeuroReport 4, 263–266.

Whaley, K., Schwaeble, W., 1997. Complement and complement deficiencies. Semin. Liver Dis. 17, 297–310.

Williams, K.C., Hickey, W.F., 1995. Traffic of hematogenous cells through the central nervous system. Curr. Top. Microbiol. Immunol. 202, 221–245.

Williams, A.E., Lawson, L.J., Perry, V.H., Fraser, H., 1994. Characterization of the microglial response in murine scrapie. Neuropathol. Appl. Neurobiol. 20, 47–55.

Williams, K.C., Corey, S., Westmoreland, S.V., Pauley, D., Knight, H., deBakker, C., Alvarez, X., Lackner, A.A., 2001. Perivascular macrophages are the primary cell type productively infected by simian immunodeficiency virus in the brains of macaques: implications for the neuropathogenesis of AIDS. J. Exp. Med. 193, 905–915.

Wyss-Coray, T., Yan, F., Lin, A.H., Lambris, J.D., Alexander, J.J., Quigg, R.J., Masliah, E., 2002. Prominent neurodegeneration and increased plaque formation in complement-inhibited Alzheimer's mice. Proc. Natl. Acad. Sci. U. S. A. 99, 10837–10842.

Yamada, T., Moroo, I., Koguchi, Y., Asahina, M., Hirayama, K., 1994. Increased concentration of C4d complement protein in cerebrospinal fluids in progressive nuclear palsy. Acta Neurol. Scand. 89, 42–46.